RIJKSWATERSTAAT COMMUNICATIONS

Nr 8

THE DESIGN AND CONSTRUCTION OF THE VAN BRIENENOORD BRIDGE ACROSS THE RIVER NIEUWE MAAS

DIRECTIE VAN DE WATERSTAAT
B2032
BIBLIOTHEEK
8

BY

IR. W. J. VAN DER EB†
Chief Engineer A of Rijkswaterstaat-Bridges Department

1968

B 2032, 8

RIJKSWATERSTAAT COMMUNICATIONS

THE DESIGN AND CONSTRUCTION OF THE VAN BRIENENOORD BRIDGE ACROSS THE RIVER NIEUWE MAAS



by

IR. W. J. VAN DER EB †

Chief Engineer A of
Rijkswaterstaat-Bridges Department

1968

Please address correspondence to

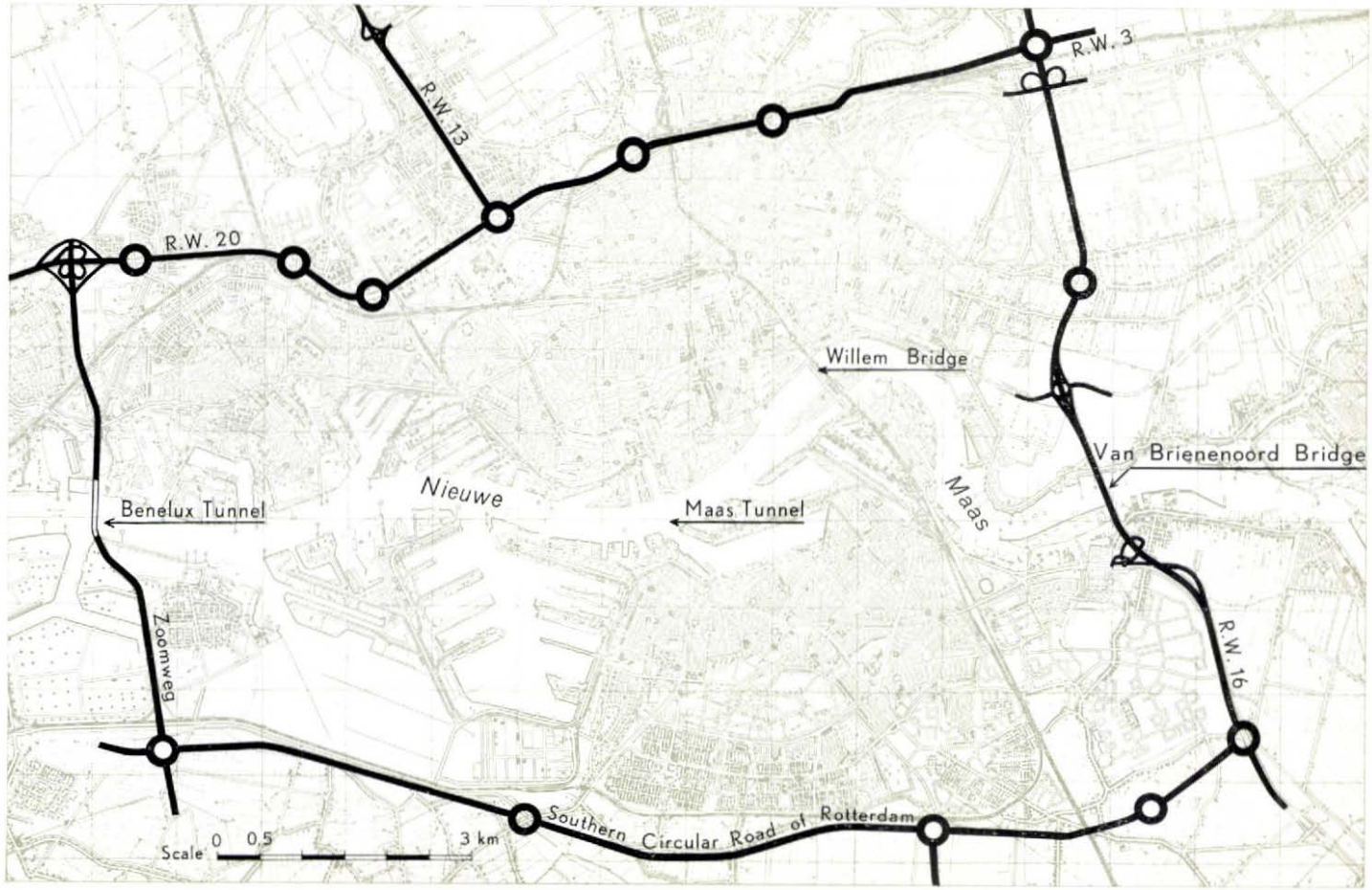
DIRECTIE ALGEMENE DIENST VAN DE RIJKSWATERSTAAT

THE HAGUE – NETHERLANDS

It is regretted that the author (designer of the bridge) died before his article could be published.
This article was completed by Ir. E. Ypey.
The views in this report are the authors' own.

Contents

page		
5	Preface	
7	Introduction	
7	Experimental and theoretical investigations	
13	Description of the bridge	
20	Calculations	
22	Erection	
30	Appendix I	The flutter theory
37	Appendix II	The vibration absorber
41	Appendix III	The orthotropic deck
50	Appendix IV	The primary longitudinal and cross girder system
55	Appendix V	The main girder system statically indeterminate to the 17th degree



Lozenge round Rotterdam with intersections.

Preface

Van Brienenoord Bridge is part of a lozenge-shaped system of roads and bridges bypassing the Rotterdam, Schiedam and Vlaardingen urban conglomeration (see opposite figure). This "lozenge" round Rotterdam was built to cope with the steady increase in the volume of traffic to and from this urban area and in through-traffic, which can now bypass it.

In 1937, Willem Bridge, over which 16,000 motor-vehicles passed every 24 hours, was the only link between the two banks of the Maas. The Maas Tunnel, the second link, was completed in World War II. In 1950, Willem Bridge and the Maas Tunnel handled 37,000 vehicles a day and by 1965 the figure had risen to 120,000. Not only was the capacity of the available traffic lines inadequate (Willem Bridge and Maas Tunnel together have only seven lanes), but the streets north and south of the river banks could no longer cope with the volume of traffic, whatever improvements were made.

In 1959, the groundwork for the first bridge in the "lozenge", Van Brienenoord Bridge, was started, followed in 1960 by the public tender for its foundations.

On 1 February 1965, H.M. Queen Juliana officially opened Van Brienenoord Bridge and the approach roads north and south of the river.

Shortly before the opening of the bridge *82,000* motor-vehicles a day were passing through the Maas Tunnel and *42,000* over Willem Bridge.

In the first week after the opening the figures dropped to *78,000* and *33,000* a day, respectively, whilst *23,000* motor-vehicles were using the new bridge daily. In May 1965 the traffic density on the bridge had increased to about 40,000 a day.

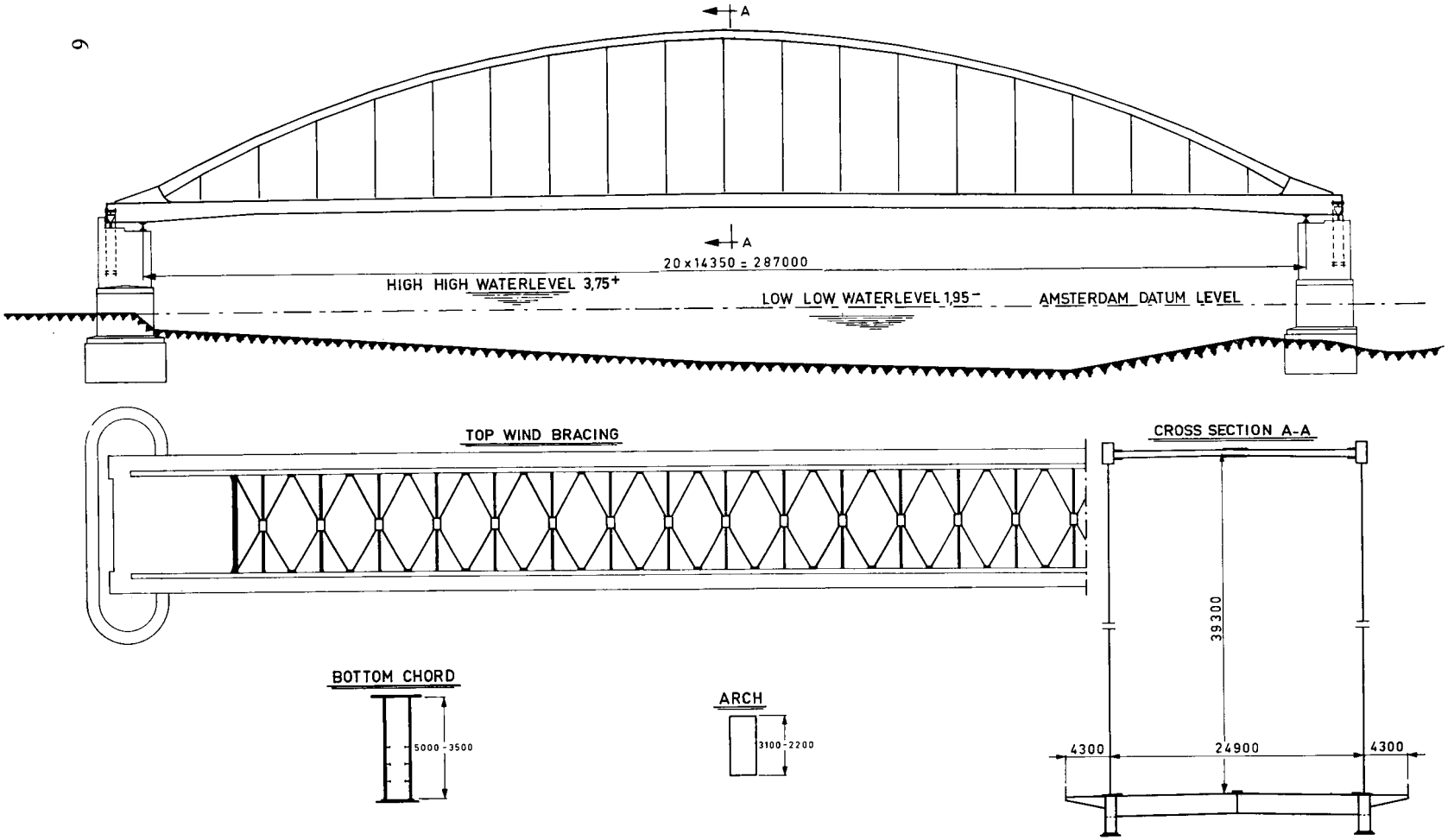


Figure 1. Scheme of original design.

Introduction

Before proceeding to describe the calculations for and the designing of the Van Brienenoord Bridge in the form in which it was finally constructed, it will doubtless be instructive and interesting, both from a theoretical and from a technical point of view, to recount what preceded the adoption of the ultimate plan. For it was not diagonal cables that were envisaged in the original scheme, but the stiffened arch type of bridge so common in Holland, with the use of cables for the vertical members and the main girders anchored to the piers so as to form fixed ends. The system adopted for instance for the bridge at Gorinchem (Figure 1).

The structure has a theoretical span of 287 metres and was first planned to be 36.5 metres wide (this was altered to 33.5 metres later), the bridge having six carriageways and two tracks 3.5 metres wide at the outer sides of the bridge for mopeds, cycles and pedestrians. It is about 40 metres high in the centre of the span and its overall length is 306.60 metres.

Experimental and theoretical investigations

The bridge is located in a windy part of the country. It is a high-level structure (bottomside of the bridge is 25 metres above Amsterdam Datum Level) and very wide; those factors, coupled with the relatively flabby stiffened arch system adopted, prompted the question whether wind-induced oscillation might cause trouble and result in the dreaded flutter phenomenon manifesting itself. The engineers had not forgotten what happened to the Tacoma Bridge, and although simple preliminary calculations using the "Amman" and "Steinman" characteristics seemed to indicate that there was no fear of flutter occurring, it was decided that windtunnel tests would be carried out at the National Aeronautical and Space Research Laboratory.

The following natural frequencies were given to the laboratory.

1. Harmonic antimetric oscillations:

a. vertical direction

unloaded: 0.62 Hertz; loaded 0.50 Hertz.

b. coupled torsional oscillations

unloaded: 1.30 Hertz and 4.89 Hertz;

loaded: 1.08 Hertz and 3.61 Hertz.

2. Harmonic symmetrical oscillations:

unloaded: 0.94 Hertz; loaded 0.75 Hertz.

The arch is not subjected to stresses during harmonic antimetric oscillation, but normal stresses will occur in it when the oscillations are symmetrical, for then $\int y.dx$ is not zero.

If we look at a cross-section of the bridge, we see that the steel orthotropic deck is monolytically attached to the top side of the two box-shaped main girders, in other

words, the two components cannot slide with respect to each other (Figure 2). The section is not symmetrical, so its centre of gravity Z does not coincide with the torsional centre M. If torsional oscillations are set up in this type of girder section, the latter will also vibrate horizontally; torsional and horizontal oscillations will be

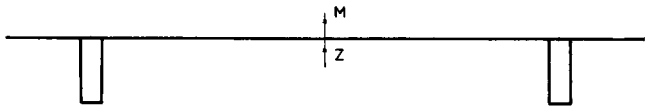


Figure 2. Cross section of bridge in outline with location of centre of gravity and torsional centre M.

mechanically coupled. This circumstance turns the flutter question into a 6th order problem (ternary system). In bridge-building it is customary to regard the flutter phenomenon as presenting a 4th order problem (binary system). For the sake of convenience Z and M are then regarded as coincident. This was still done fairly recently in experiments carried out in Germany.[1])

The binary system is adhered to in these investigations, both theoretically and experimentally. Theoretically, the spring supports are in that case as shown in Figure 3.

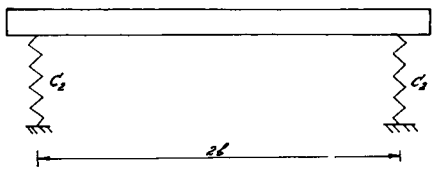


Figure 3. The system of spring supports customary with flutter investigations.

The ternary system was taken as the problem in both the theoretical and the experimental investigation for the Van Brienenoord Bridge. The theoretical treatment of the 6th order problem arising therefrom is given in Appendix I. There is no doubt that a characteristic 4th order equation is easier to discuss than one of the 6th order.

The use of electronic computers have made it much easier to overcome the difficulties of the theoretical investigations.

In the experiments the three degrees of freedom and the mechanical coupling between torsional and horizontal oscillations are taken into consideration by the use of an unconventional system of spring supports as shown in Figure 4. A high degree of accuracy was attained therewith when reproducing the actual characteristics of the bridge.

---

[1]) „*TEILMODELLVERSUCHE ZUR BEURTEILUNG DES AERODYNAMISCHEN VERHALTENS VON BRUCKEN*", von K. Klöppel und G. Weber, Darmstadt.
DER STAHLBAU, 32. Jahrgang / Heft 3 / März 1963 / p. 65–79.
DER STAHLBAU, 32. Jahrgang / Heft 4 / April 1963 / p. 113–121.

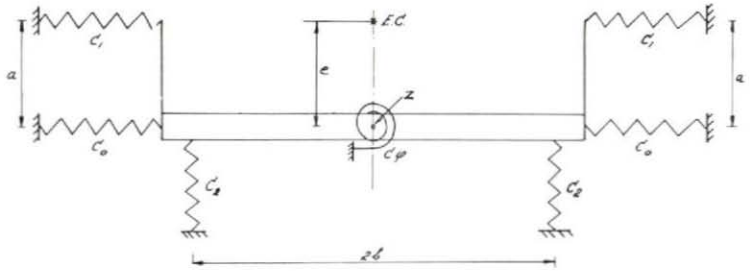


Figure 4. The system of spring supports used with the flutter investigations for the Van Brienenoord Bridge, taking into consideration the ternary system.

The wind-tunnel tests were carried out on a wooden model (scale 1 : 100) representing the actual structure as closely as possible. First of all, the atmospheric forces acting on the model were measured; then came the actual flutter test.

The wooden model (see Figure 5), scale 1:100 is 80 cm long, 33.5 cm wide and 3.15 cm high. So it represents a section of bridge 80 m long.

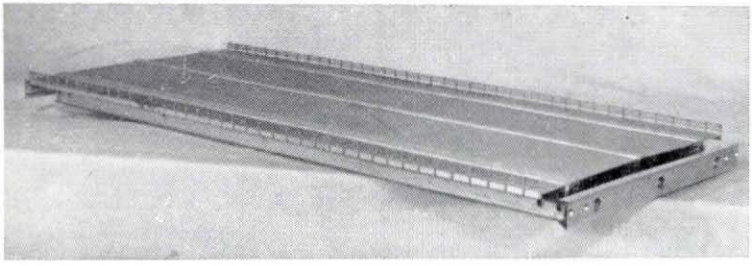
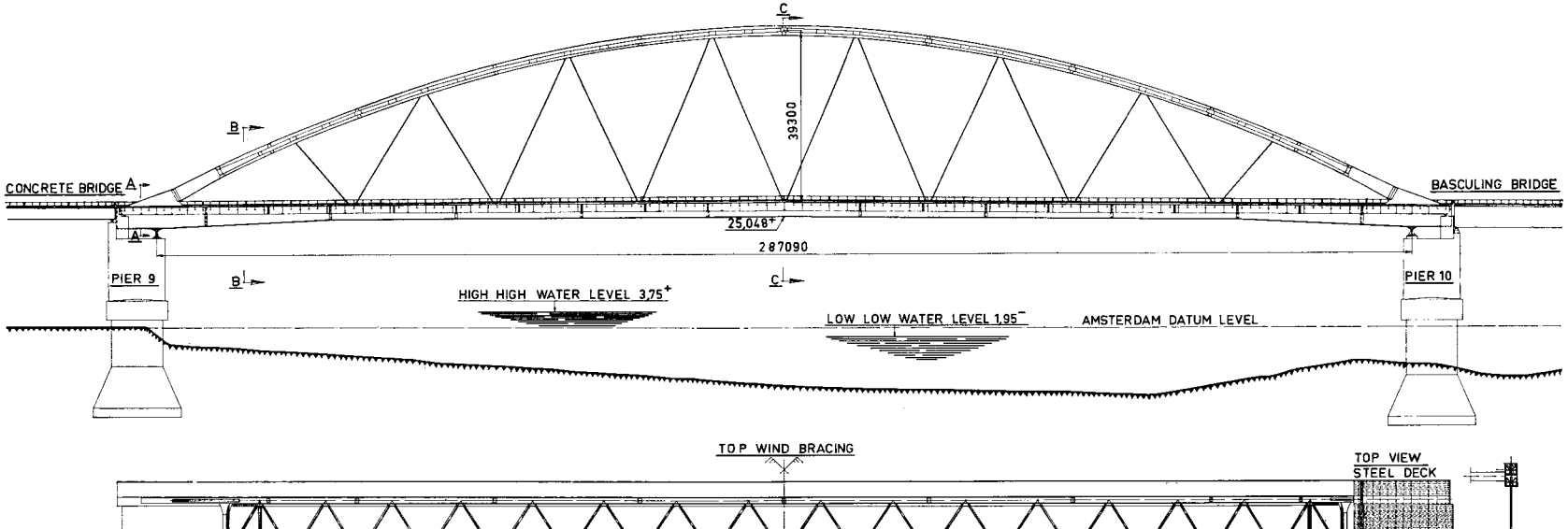


Figure 5. Photograph of model.

The following summary is taken from the report received.

"Experiments have been conducted to discover whether the Van Brienenoord Bridge will be susceptible to flutter. The atmospheric forces acting on a model of the bridge were measured in the wind tunnel and a flutter test was carried out. It appeared that there was no danger of actual fluttering but that the bridge can develop an oscillation of limited amplitude due to the occurrence of 'Kárman vortex streets'. Both bending and torsional vibrations can occur. The results of the experiments show that only the bending oscillations are of any consequence to the bridge, since they lie within the range of wind velocities that are likely to occur. The stresses that the bending oscillations may set up in the structure were arrived at by deducing from the results of the tests the magnitude of the force exerted by the atmosphere on the bridge to set it vibrating. The damping system proposed by client will be capable of keeping these oscillations down to reasonable proportions."

Accordingly, there was no danger of flutter occurring; the oscillations of limited



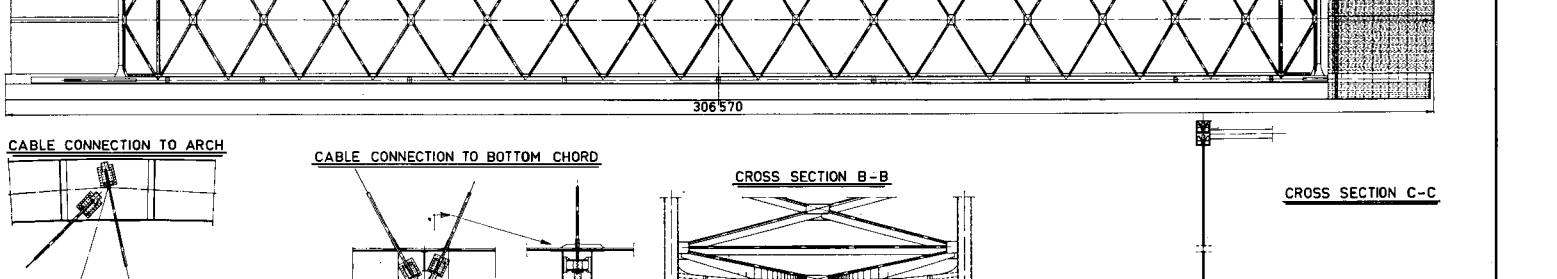


Figure 6. Scheme of the final design.

amplitude were serious enough, however. The latter can be regarded as periodic loading in the resonance zone.

Oscillations of limited amplitude occurred at two wind velocities, viz. 61 km p.h. and 93 km p.h. (7 Beaufort and 10 Beaufort, respectively).

The periodic forces to be anticipated must be fixed at 13.6 Kgs per metre and 44.1 Kgs per metre of the main girder.

Damping tests had been made on another steel bridge. Adapting the results of these tests to the dimensions of the Van Brienenoord Bridge it was concluded that a dynamic amplification factor of about 110 could be anticipated (K = 5,000), which would give an equivalent static loading of about 4.8 tons per metre per main girder. If a gust should last long enough to allow the resonance phenomenon to develop completely, a stress of about 1,600 Kgs per square centimetre would occur in the structure.

Obviously, this could not be tolerated.

Two remedies suggested themselves, viz.

1. Adoption of the diagonal-cable design; there were aesthetic objections to this, because to the eye it meant reversion to the truss girder type;
2. incorporation of what is called a dynamic oscillation absorber.

After these tests, first the desire had been expressed to retain the stiffened arch design with vertical cables, therefore calculations for the oscillation absorber were completely worked out and designed first. The mathematical aspect of the device is dealt with in Appendix II.

It was found that four 13.75 ton weights (1.75 cub.m. of steel each) could give the characteristics described in Appendix II for a maximum oscillation of 15 cm.

An absorber of the flow-pattern type was the one adopted. The springs required could be manufactured and would be sufficiently resistant to metal fatigue. So the system was reasonably feasible; wind tunnel tests had proved it. Be that as it may, an oscillation absorber is a device that needs constant maintenance if it is to remain effective. It would be looked after well enough for the first few years, but it would be gradually forgotten and neglect would render it ineffective at a certain moment.

It was partly owing to those objections against absorbers on the score of maintenance but mainly owing to the architect's favourable verdict on diagonal cables that opposition to the designer's preference for a bridge with diagonal cables was overcome.

Thereupon it was decided that this design should be worked out.

It resulted in:

1. a saving in weight of about 500 tons;
2. a minimum natural frequency of 1.3 Hertz instead of 0.62 Hertz, while the natural frequencies of the deck, at which practically no arch stresses would occur by vibration, rose from 0.62 Hertz unloaded and 0.50 Hertz loaded to 7.68 and 6.12 Hertz, respectively.

Accordingly, the mechanical properties of the design proved to be much better.

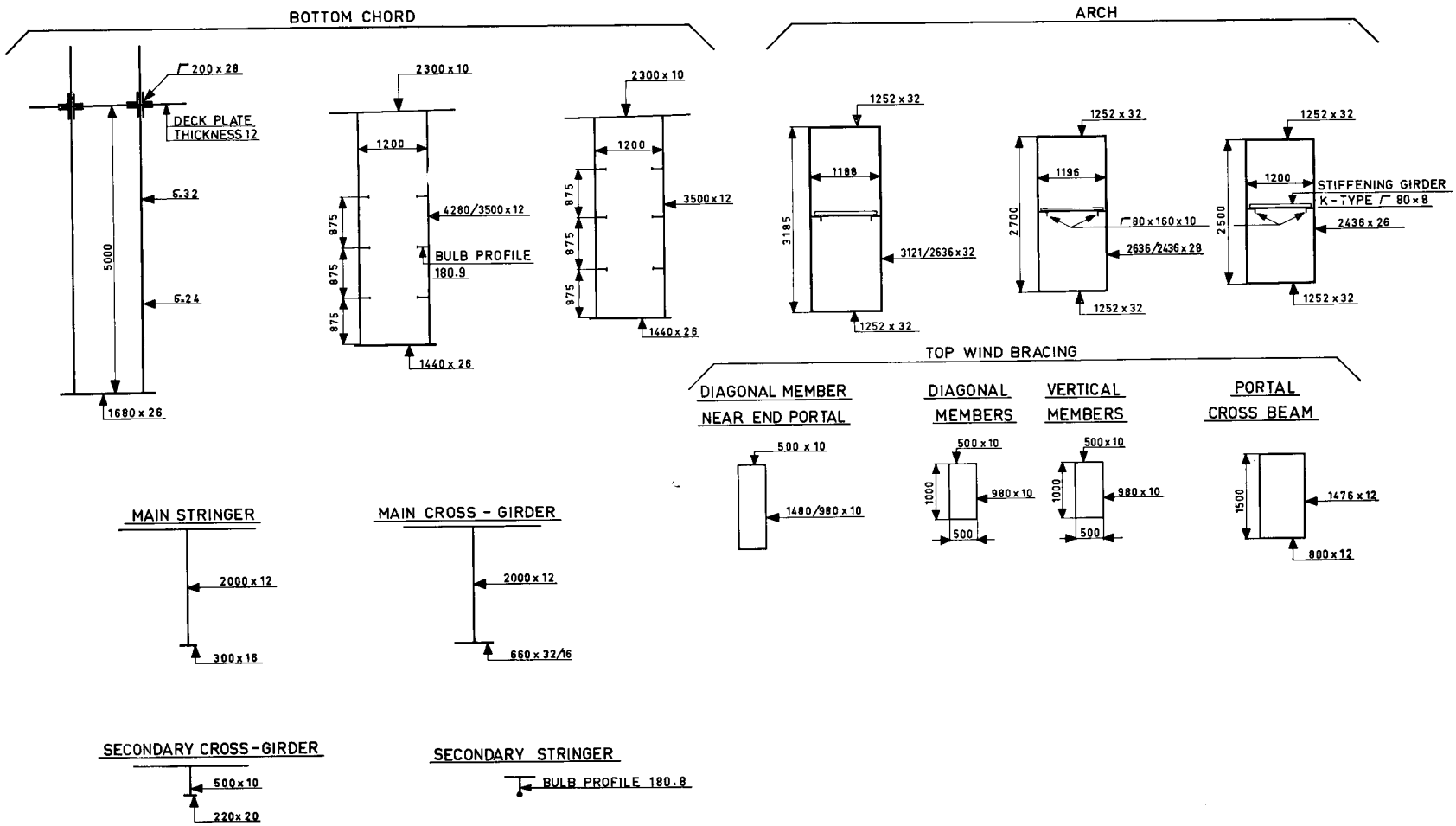


Figure 7. Cross section of component parts.

The diagonal-cable design was adopted in the end and practically everyone is now reconciled to the idea of having the diagonal cables.

Description of the bridge

Figure 6 shows the bridge as finally constructed. Each of the main girders consists of a rigid box-sectioned bottom chord and arch rigidly attached to each other at their extremities by means of gusset plates. Diagonal suspension members stretch from arch to bottom chord; they are made up of single-rope suspension bridge cables. The cables are attached to arch and bottom chord by means of cast steel saddles.

The end portals of the bridge are in the plane of the arches. They merge into the rhomboid lattice-girder wind bracing linking the arches. The main members of this wind bracing are also of boxshaped section.

Contrary to the eccentric connection of top wind bracing to top chords usually adopted in Holland, the top wind bracing of the Van Brienenoord Bridge is correctly attached to the arch members, the centre lines of the members being situated in the same plane as the centre-line of the archmembers, in this way reducing the secondary stresses.

The bridge deck is constructed as an orthotropic plate and is attached between the bottom chords of the main girders. The structure of this deck differs entirely from all the other orthotropic decks made in Holland up to this time, for it is designed on the subdivision principle.

It consists of the primary longitudinal and cross girder system with the secondary units in between. The main stringer, designed as a continuous beam, runs down the centre of the bridge and extends throughout its length. It is supported every 14.35 metres by main cross girders extending the entire width of the bridge between the main girders. The main stringer and the main cross girders are 2.05 metres deep. The dimensions of the component parts can be read off in Figure 7.

Accordingly, the secondary cross girders only span half the width of the bridge between the main girders. They are 0.52 m deep. The secondary stringers consist of bulb sections spanning the 2.05 m between the secondary cross girders and are welded to the deck plate at 30 cm intervals.

At the location of the supports of the bridge there are three main cross girders closely spaced, the girders being attached to the main girders with the use of triangular bracket plates. These three cross girders are forming also the bottom chord of the end portals of the top wind bracing. All the lateral forces are ultimately transferred to the supports through this part of the portal (Figure 8).

The thickness of the deck plate is 10 mm except at the ends of the bridge where the arches are connected to the main girders. Here the deck thickness increases to 24 mm at each side of arches over a width of 1.10 metres and a length of 20.22 metres. The purpose of the thickening is to transfer the horizontal components of the arch forces to the deck.

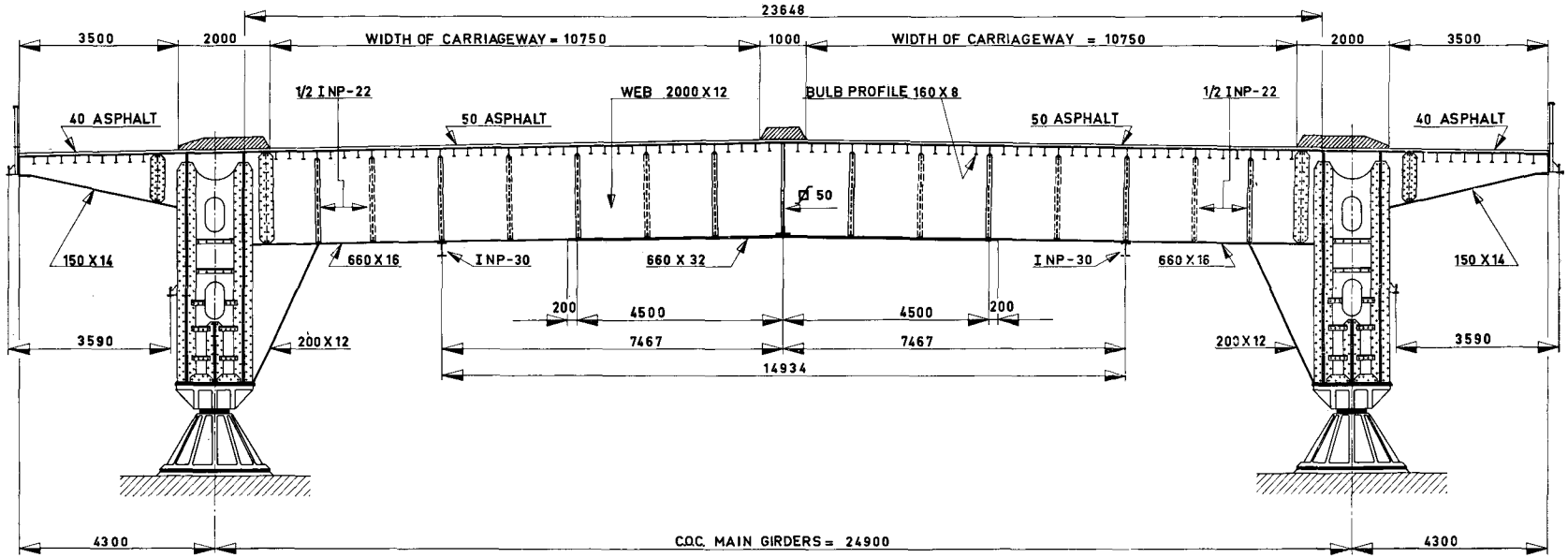


Figure 8. Cross section of bridge above the supports.

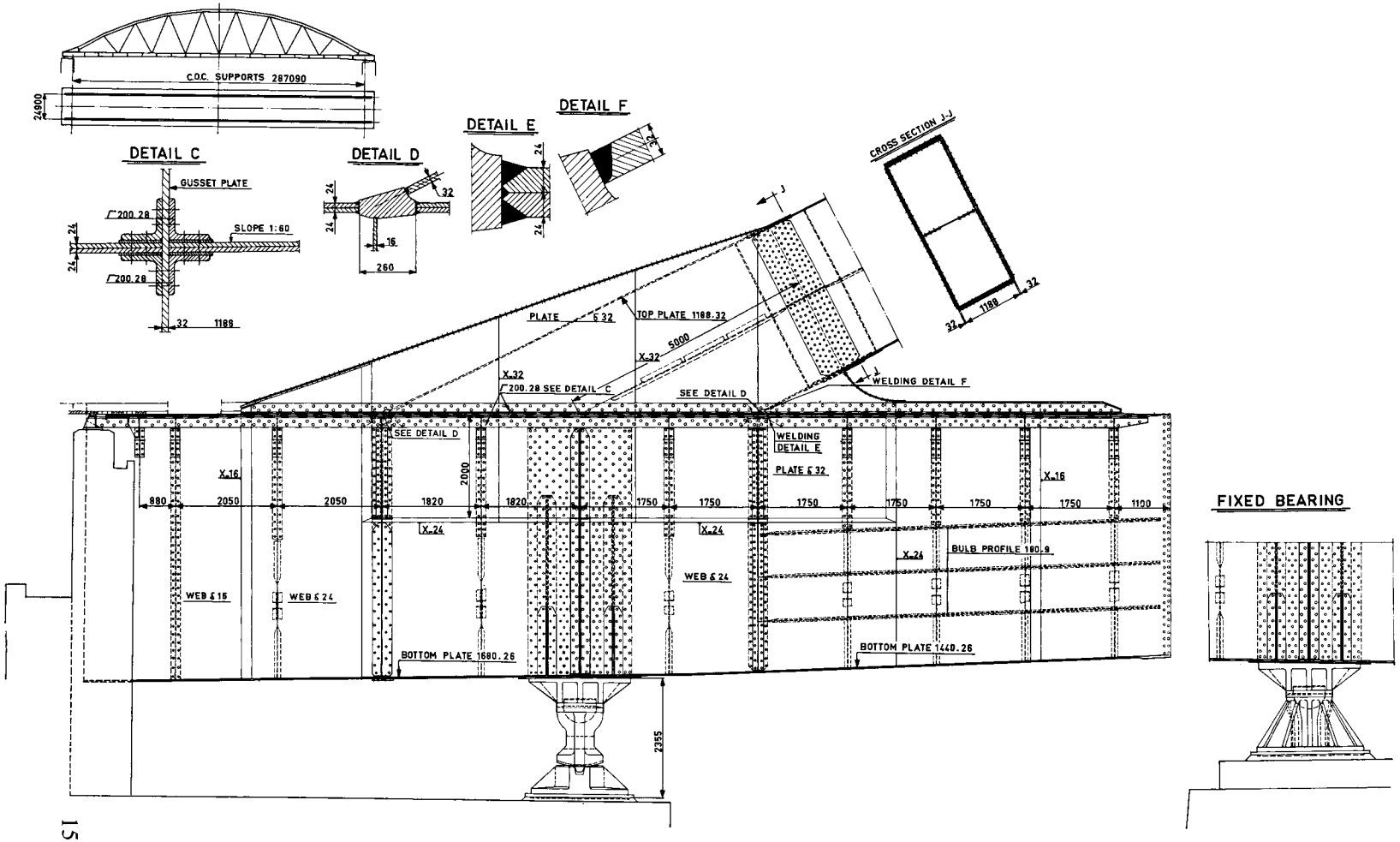


Figure 9. Connection arch to bottom chord with supports.

The cross-section of the arch increases considerably towards each end, because the latter forms part of the end portal and as a result of that is subjected to a not inconsiderable bending moment in addition to the normal force in the arch.

The webs of the bottom chords, which are 12 mm thick, are provided with three bulb-sectioned longitudinal stiffeners. These stiffeners being required in order to prevent buckling of the webs during erection of the bridge. There are also transverse stiffening plates inside the bottom chords at the connection of each cross girder, that is at every 2.05 metres.

The arch members are internally provided with transverse plates and a stiffening girder. The K-shaped stiffening girder running the entire length of the arch is attached halfway up the section in order to ensure that the webs of the arches shall have adequate resistance to buckling. The interiors of both the arches and the main girders are completely accessible.

Figure 9 shows the connection of arch to bottom chord in detail. The thickness of the two webs increases from 12 mm to 32 mm over half the height of the bottom chord, which is 5.5 metres deep at the point of support. These plates can be regarded as gusset plates. The thickness is gradually reducing from 32 mm to 24 mm, then to 16 mm, whence it reaches normal web thickness. The ends of the arches are 3.5 metres high, so the end connection is about 9 metres high, measured from the base to the top of the gusset plates. The end connection structure, 21.20 m long, was delivered to the site entirely completed.

The diagonal cables are 110 mm dia. suspension bridge cables with a breaking strength of 180 Kgs per square millimetre.

Cable shoes are attached to each end of the cable with the use of white metal. The weight of the bridge deck is such that only tensional forces will occur in the diagonals; the cable load varies from + 70 tons to + 320 tons.

The erection joints between the various sections and all the joints between cross girders and main girders are riveted. Riveting was deliberately adopted for the erection joints in order

1. to keep shrinkage stresses due to electric welding within reasonable limits;
2. to enhance the internal damping capacity of the structure.

For riveted joints dissipate energy internally much more readily than the material itself (resonance when oscillating).

Figures 10, 11 and 12 show some other details of the bridge.

The bridge decking has received an asphaltic wearing surface consisting of the following layers:

a. a sealing coat made of fluid bitumen 150/250 with a volatile solvent

b. an adhesion layer consisting of:

fluid bitumen 150/250	95 weight per cents
pulvatex rubberpowder	5 weight per cents

weight of layer 0.8 – 1.0 kgf/m² surface

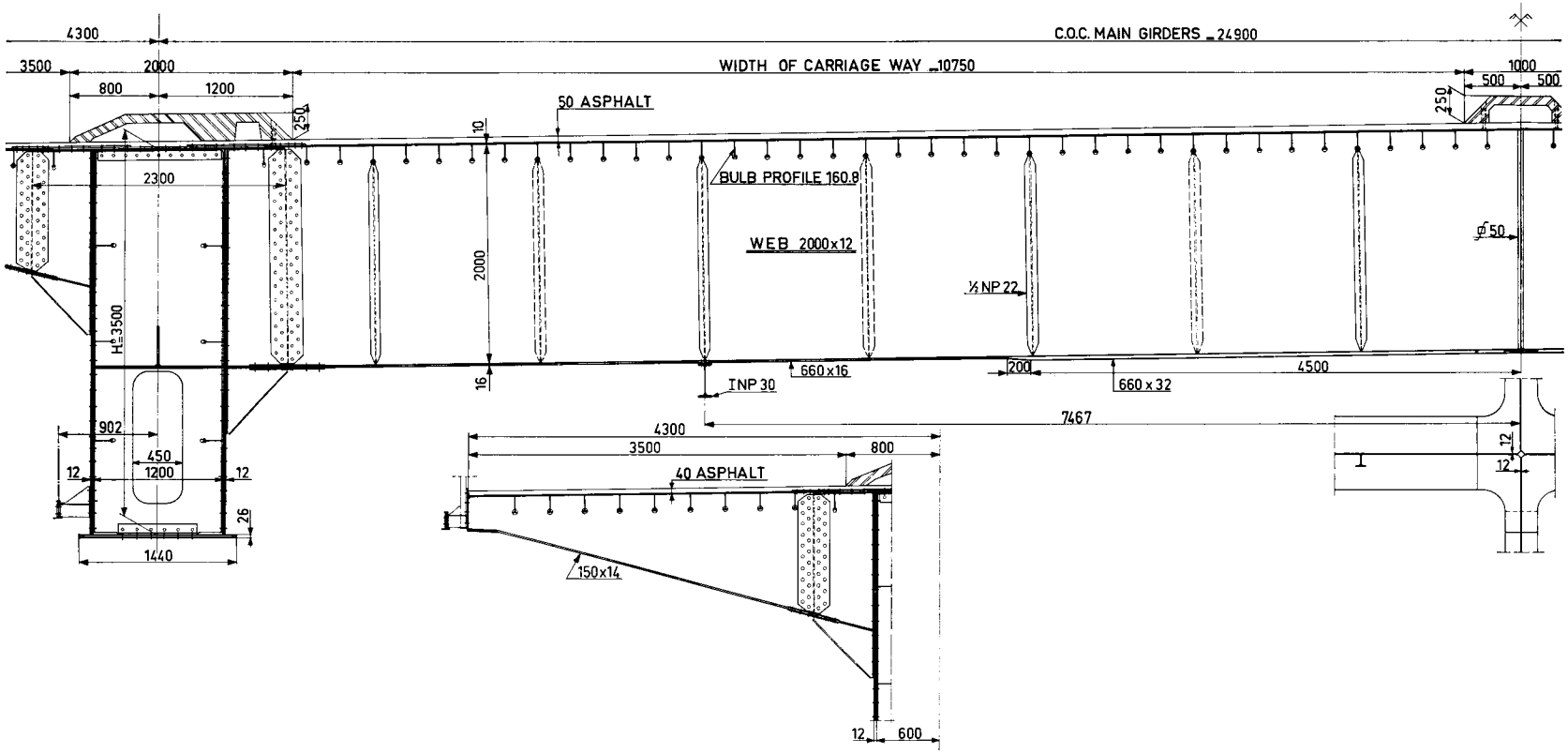


Figure 10. Main cross girder.

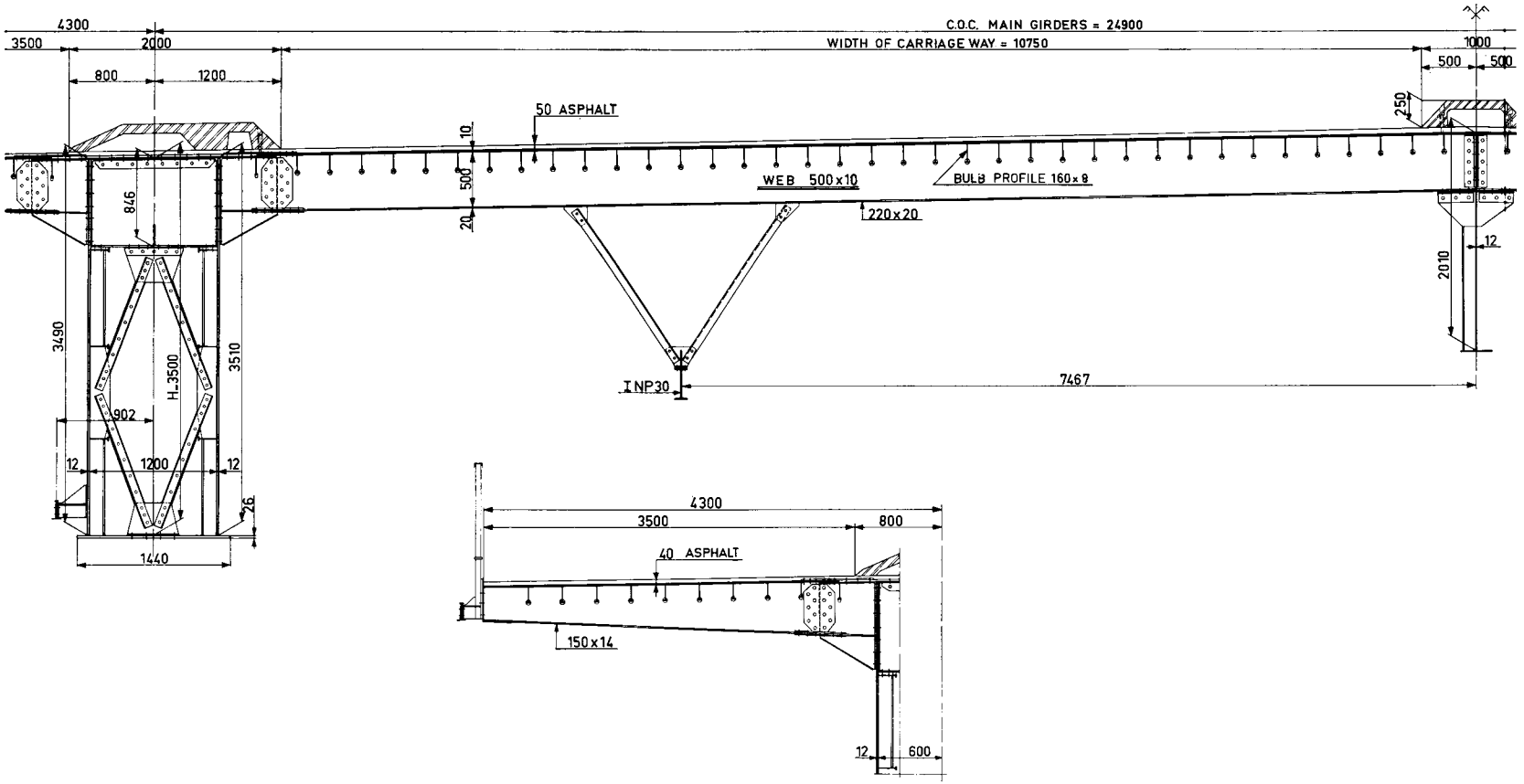


Figure 11. Secondary cross girder with suspension construction for track of inspection car.

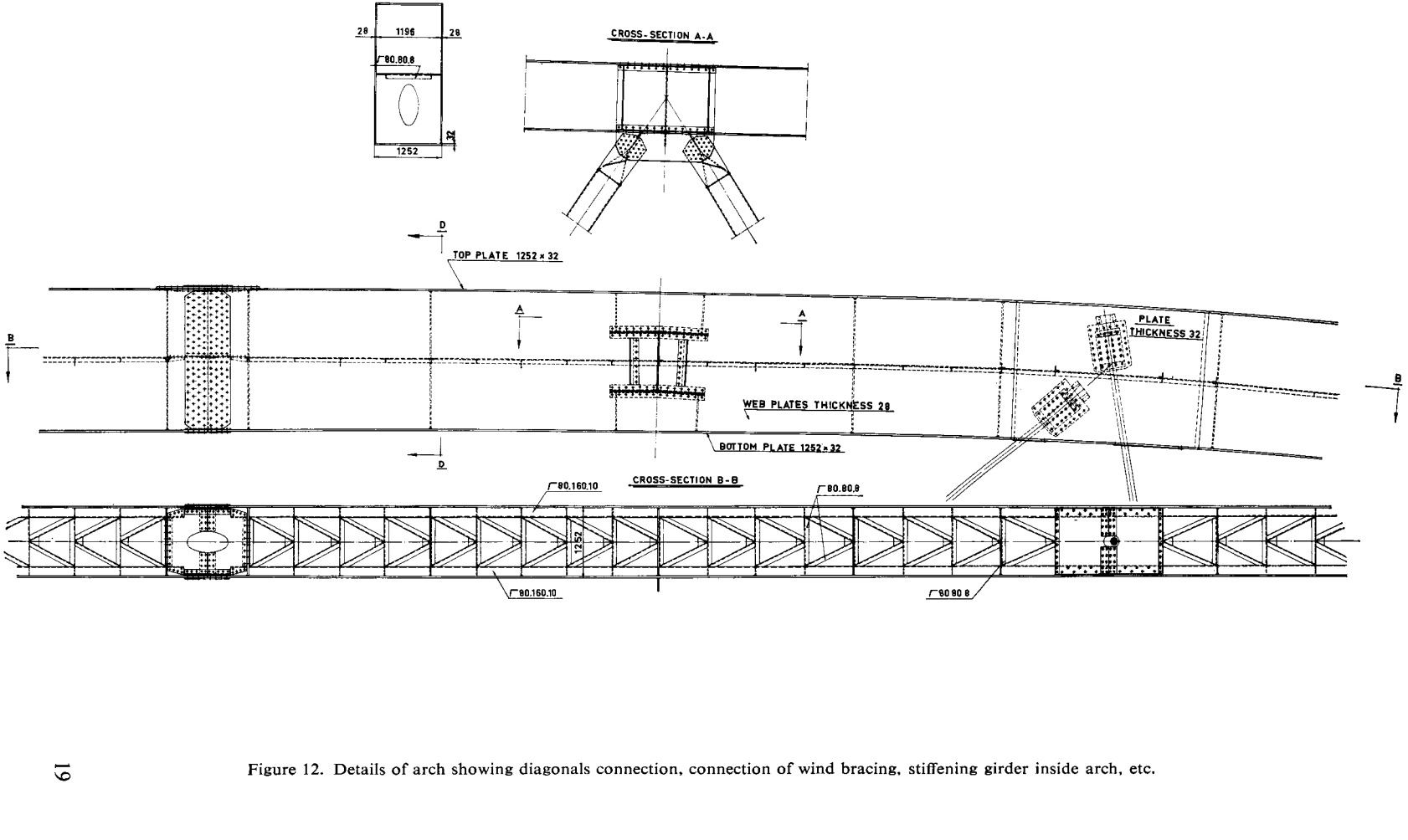


Figure 12. Details of arch showing diagonals connection, connection of wind bracing, stiffening girder inside arch, etc.

c. a mastic layer with a thickness of 8 mm consisting of:

river sand	19	weight per cents
dune sand	19	weight per cents
limestone filler	47	weight per cents
asphalt bitumen 40/50	15	weight per cents

d. an intermediate layer of melted asphalt with a thickness of 20 mm consisting of:

fine gravel	35	weight per cents
river sand	15	weight per cents
dune sand	15	weight per cents
limestone filler	26.5	weight per cents
asphalt bitumen 40/50	8.5	weight per cents

e. a top layer of melted asphalt with a thickness of 22 mm consisting of:

gravel 2-5 mm	40	weight per cents
river sand	22	weight per cents
dune sand	11	weight per cents
weak filler	16	weight per cents
asphalt bitumen 50/60	5.5	weight per cents
Trinidad asphalt	5.5	weight per cents.

Total thickness of the wearing surface 50 mm.

Three firms were commissioned to fabricate the bridge, viz.

1. Main contractor: Braat N.V., at Rotterdam for the arches and moped tracks;
2. Werkspoor N.V., at Utrecht for the bottom chords and end connections;
3. N.V. Pletterij v/h L. I. Enthoven & Cie, at Delft for the orthotropic deck between the bottom chords.

The bottom chords and the deck in between were assembled at the Pletterij yards situated on the banks of the river Hollandsche IJssel near Gouderak 10 miles north-east of the building site. The members were fitted together free of stress with the prescribed erection camber, the rivet holes reamed and bridge section by bridge section, two bottom chord members and deck members riveted together. The rivet holes for the erection joints between the bridge sections were also reamed, but were only secured with pins and bolts during assembly at the yard.

Calculations

The calculations may be divided up into the following main groups.

1. Those for the orthotropic deck itself, divided up into sections and lying between the primary longitudinal and cross girders;
2. those for the primary longitudinal girder (main stringer), flexibly supported by the primary cross girders. All the cross girders being attached at both ends to the main

girders who have a torsional rigidity and as a result of that produce bending moments at the ends of the cross-girders, when these girders are loaded;

3. those for the main girder (arch top chord, horizontal bottom chord and diagonals combined), which is statically indetermined to the 17th degree.

The girder was calculated exactly with the aid of influence lines, due account being taken of all the deformations due to the elongations of the diagonal cables;

4. those for the portals and the wind bracing (between the arches);
5. various calculations of the details of the bridge.

The mathematical formulae underlying these calculations will be found in the various appendices, with the exception of the calculations for 4 and 5, which are not given, as they would take up too much space.

As regards 4, it is interesting to note that the portal crossbeam has been given large dimensions only for the sake of appearance. Bending stresses hardly act on the beam at all, because of the tremendous dimensions and stiffness of the arches, which transmit most of the wind forces direct from the wind-bracing to the end cross-girders.

One of the detail calculations was that to calculate the stress in the deck at either end of the bridge at the locations where the forces from the arches were introduced; they were computed with the aid of Airy's stress function.

Weights and Dimensions

Main girders	1,500	metric tons Fe 52
Deck between main girders	1,425	metric tons Fe 52
Moped tracks	306	metric tons Fe 52
Arches	1,228	metric tons Fe 52
Wind bracing and portals	332	metric tons Fe 37
Total structural steel	4,791	metric tons
Diagonal cables	86	metric tons Fe 180
Parapets	40	metric tons Fe 37
Painters' car and track	72	metric tons Fe 37
Inspection paths	15	metric tons Fe 37
Total	127	metric tons
Fixed supports 2×20 metric tons	40	metric tons Cast Steel Fe 52
Roller supports 2×28.5 metric tons	57	metric tons Cast Steel Fe 52
Total	97	metric tons

Theoretical span	287	metres
Total length	306.6	metres
Total width	33.5	metres
Total area	10,271	square metres
Weight per running metre of bridge structure	16.00	metric tons
Weight per square metre of bridge structure	475	Kgs per square metre

Erection

At first, the stipulation that there might only be two temporary supports in the river due to the heavy navigation, presented no simple problem. Figures 13 and 14 show the erection plan finally decided upon, which made it possible to build the structure without strengthening the bridge at all. Contrary to the usual procedure of leaving the planning of erection operations to the contractor, the erection plan and most of the appliances, such as the temporary towers, needed for the Van Brienenoord

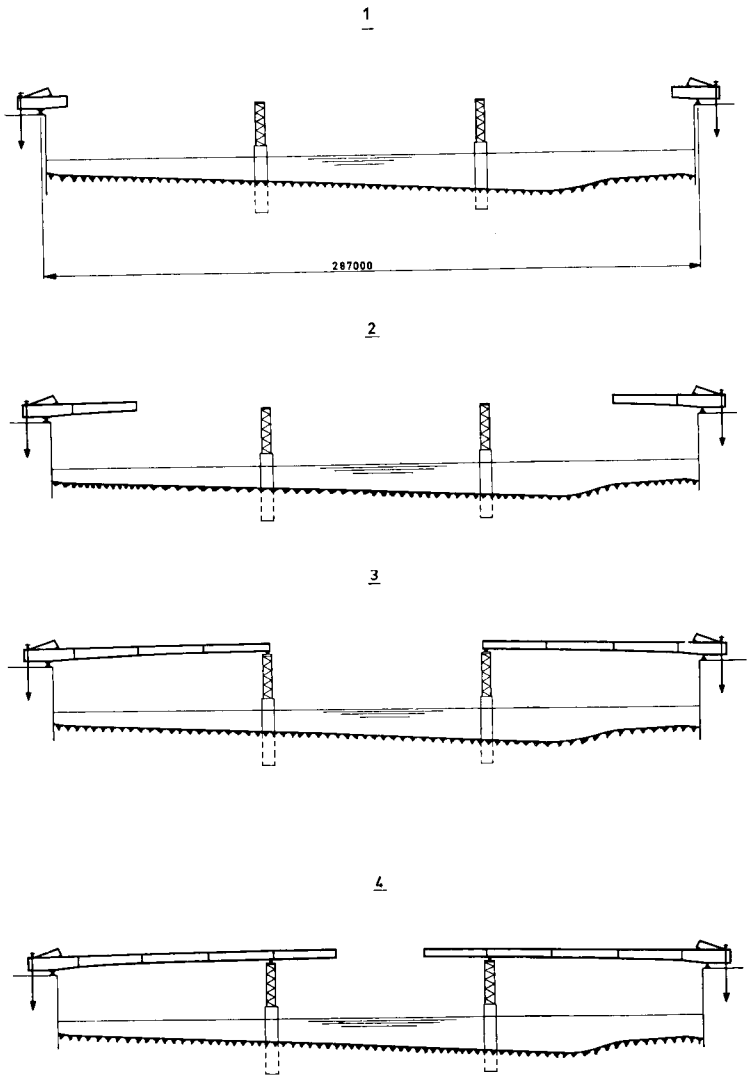
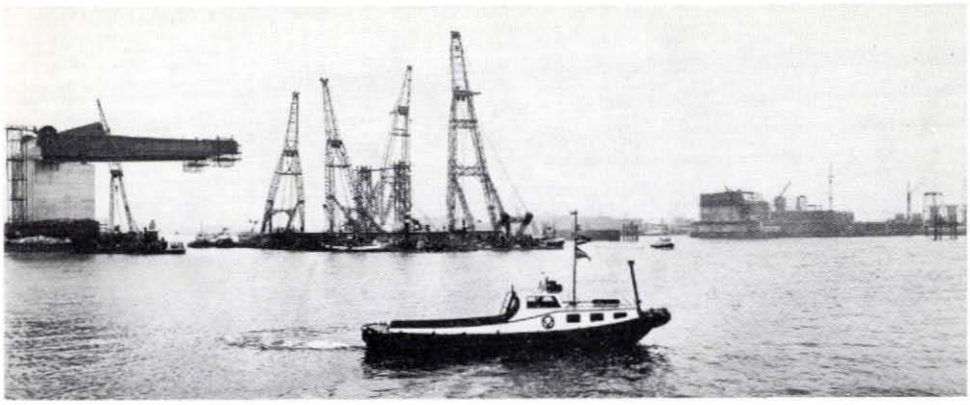
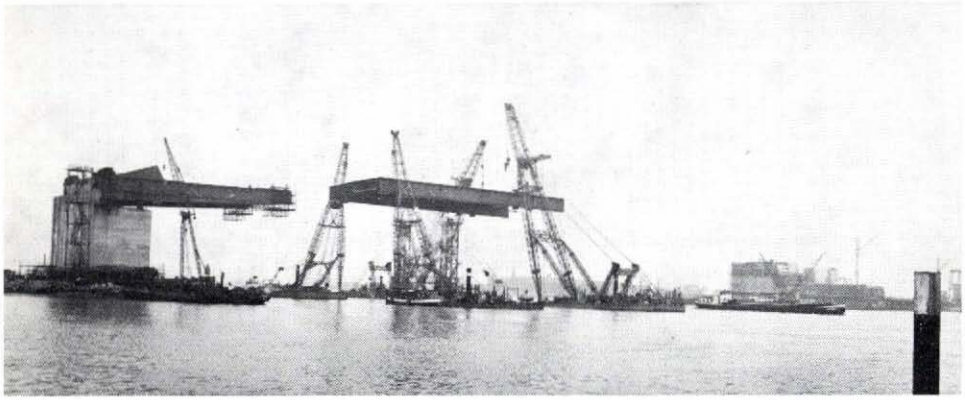


Figure 13. Scheme of the erection of the bridge deck construction.



Photograph 1. Placing the 56 metres long and about 500 tons weighing double bridge section. The first bridge being erected and fixed to the pier, the double bridge section still laying on the barges.



Photograph 2. The double bridge section lifted 30 metres but not yet connected to the first bridge section.



Photograph 3. The erection of the bridge deck completed as well as erection of the first lifting towers for the arches.

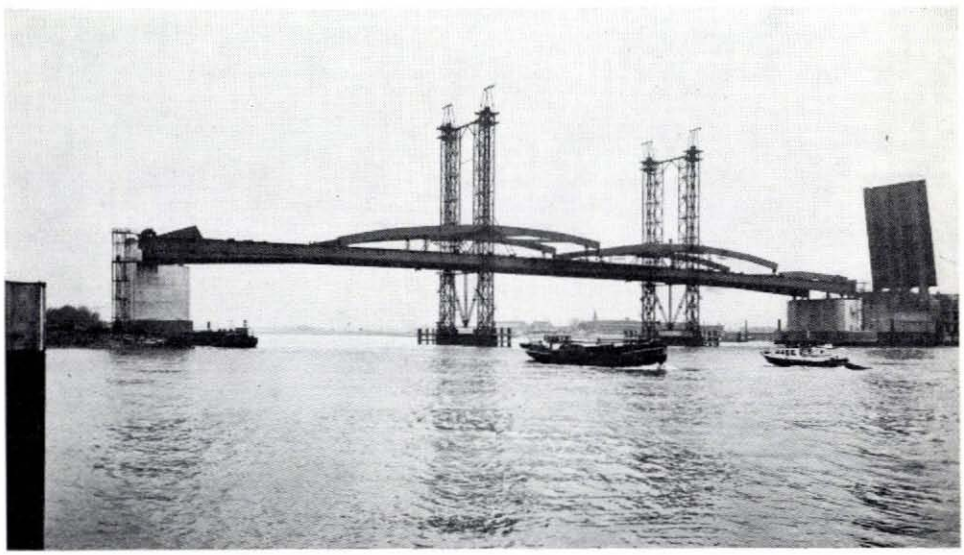
Bridge were worked out by the Bridges Department of Rijkswaterstaat and made obligatory to the contractor.

Advantage was taken of the opportunity to anchor the heavy main girders to the concrete pier; that was the permanent method of construction intended in the original design of the stiffened arch bridge with vertical suspension cables, but in the new design it was only to be adopted to make a cantilever erection method possible.

The first bridge section built both southwards and northwards was erected in three separate parts – the two end sections of the bottom chords and the deck structure (Figure 13-1). All the other bridge sections were jointed when entirely complete – two bottom chords and the deck between them, which had been riveted together in the assembly yard (Figure 13-2). In two cases two bridge sections riveted together were actually erected as one piece (Figure 13-3). That had to be done to obviate the necessity of temporarily stiffening the horizontal girders and the anchoring structure, the temporary pier thus being reached in a single operation, considerably relieving the structural elements of the first section. Placing the 56 metres long sections weighing about 500 tons was undoubtedly a spectacular undertaking; they had to be raised about 30 metres and were placed with the use of four floating cranes. Fortunately, both operations were accomplished without a hitch.

When the entire horizontal bridge structure was completed, the erection started of the lifting towers for the arches. When they were completed, the erection of the arches could start.

The order in which the various operations of this erection were carried out is shown clearly in Figure 14. First the sections of the arches together with the top wind bracing



Photograph 4. Assembling the arch sections on the bridge deck.

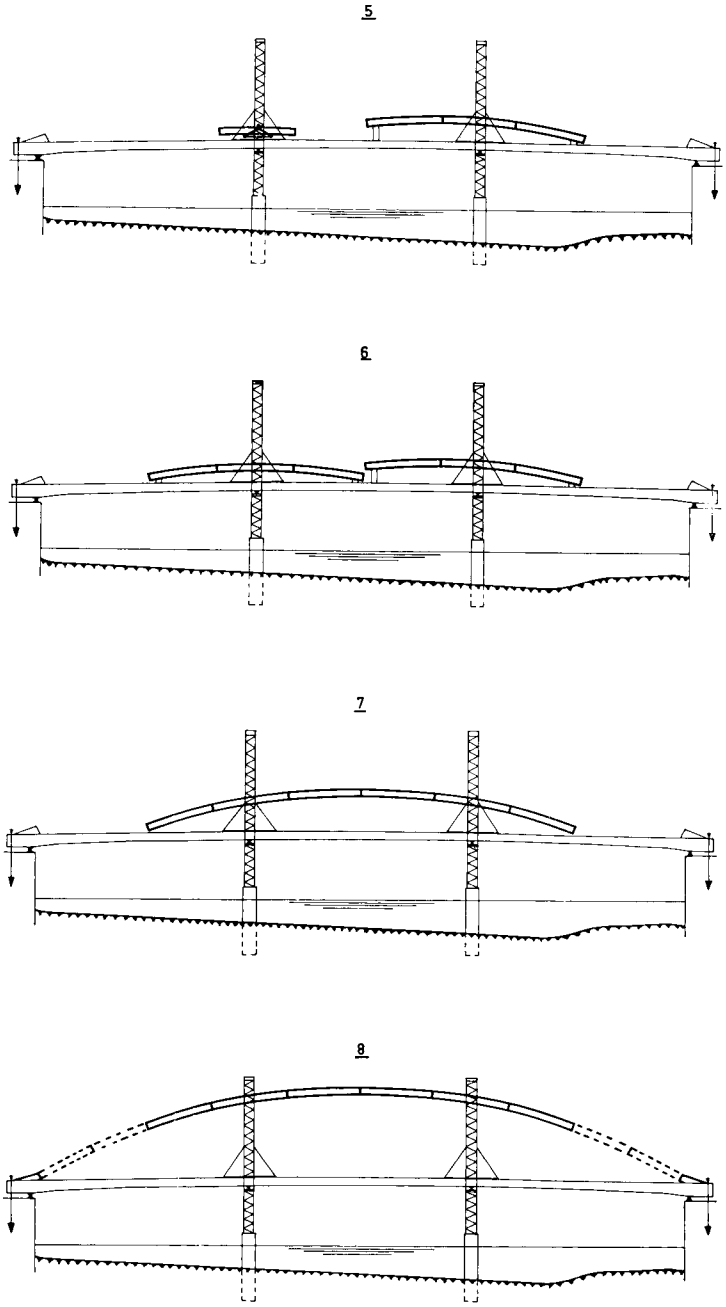
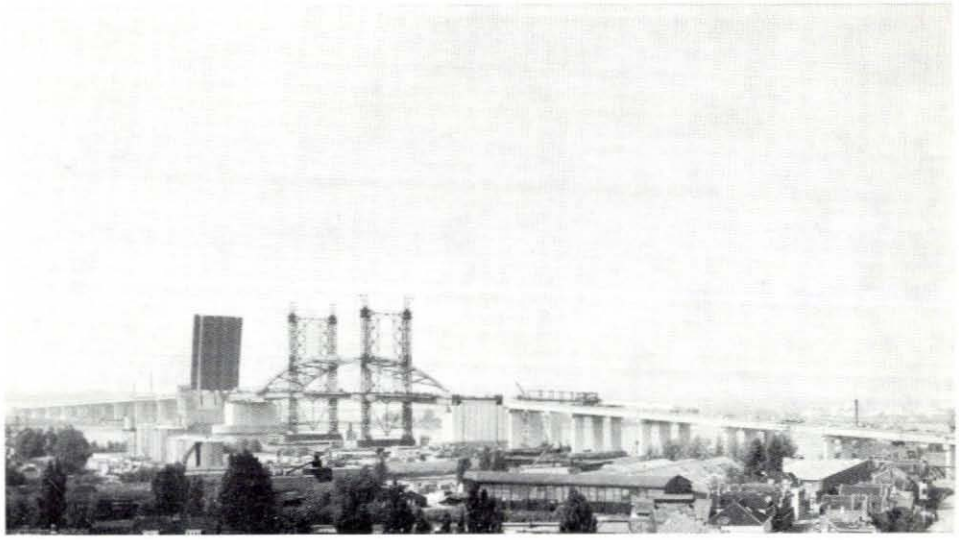


Figure 14. Scheme of the erection of the arch and top wind bracing.



Photograph 5. Lifting of the arch sections.

were placed on the bridge deck and assembled to two larger sections each consisting of three arch sections and the top bracing in between (Figures 14-5 and 6). The two halves of the arches were then partly lifted and linked together at the top and the entire assembly riveted, including the wind bracing between the arch sections. The entire structure weighing 1,200 tons was then lifted up (Figures 14-7 and 8). Jacking rigs made up of 5.25 metres long strips, hinged together, were used for the purpose. The actual jacking was done with a double jack system consisting of two sets of two jacks on each lifting tower, each jack having a lifting capacity of 350 tons. The strips were drilled to take pins so that the step-by-step jacking method could be used.

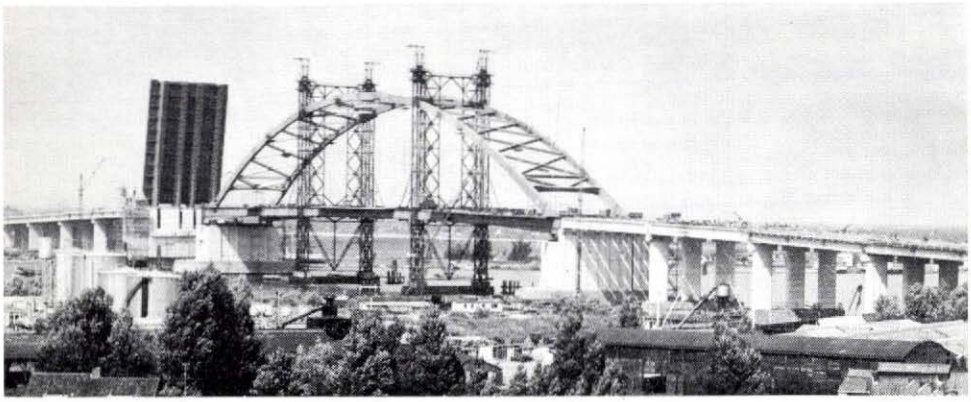
When this arch section had been raised to the correct height on the temporary piers the four extremities of the section were jacked up to its ultimate position with the use of telescopic masts. Then the four remaining sections of arch were assembled. Only slight adjustment of the anchors on the piers was required to make the sections link up with the end gussets.

Next, the diagonal cables were fitted. They hung loose between their points of attachment, because the bottom chords had been given excessive camber. When the moped tracks outside the main girders were in position, the bridge deck assembly was lowered, causing the cables to straighten and take the weight of the bridge deck.

Finally, after the asphalt deck had been laid, there were a few wind-bracing gussets to ream and rivet; they had purposely been left till the last to ensure that the secondary stresses set up in the arch by the rhomboid lattice-girder bracing should be kept as low as possible.



Photograph 6. Lifting of the arch sections.



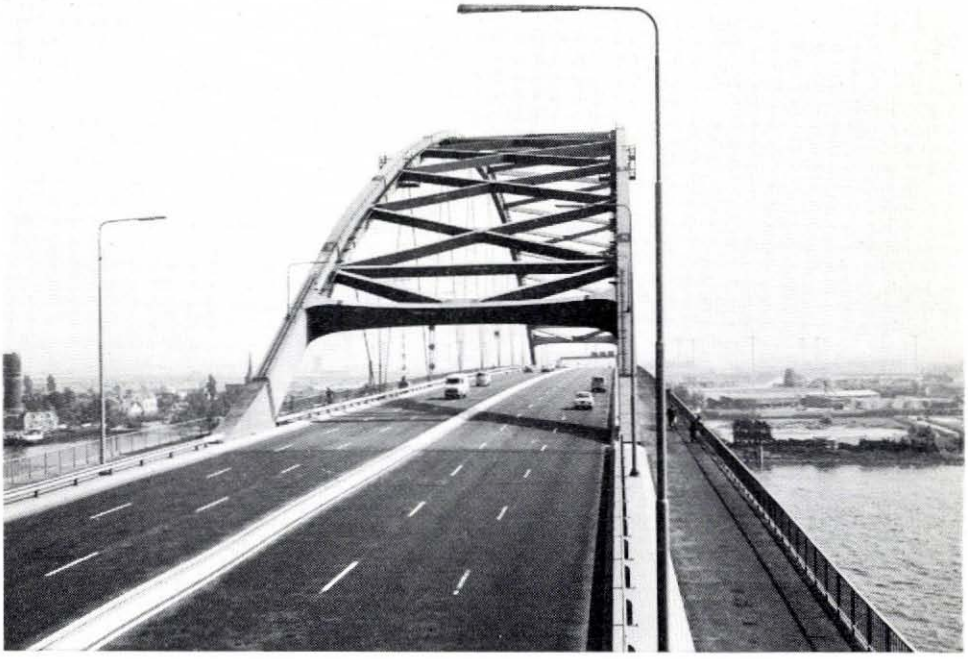
Photograph 7. Erection of the arches completed.



Photograph 8. Erection of the arches completed.



Photograph 9. The erection of the bridge completed. Removing of temporary pier constructions.



Photograph 10. The bridge completed.

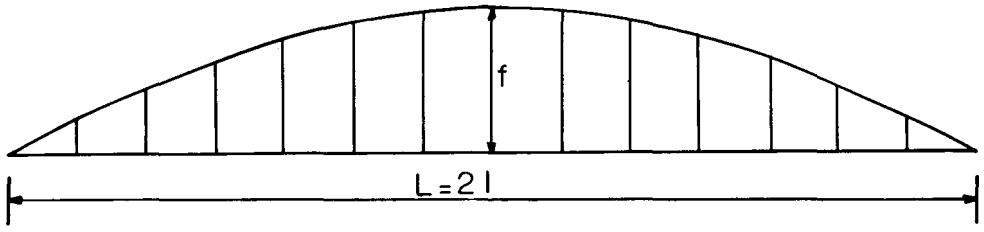
Note on Appendices

Needless to say, the following mathematical deductions had to be kept as concise as possible, in view of the limited space available. Accordingly, many of the intermediate stages have been omitted.

Appendix I The flutter theory

List of notations

EI_v = flexural rigidity in vertical direction
EI_h = flexural rigidity in horizontal direction
EC = warping rigidity
GI_p = Saint Venant torsional rigidity
m = mass of girder per unit of length
θ = mass moment of inertia of girder in relation to its axis of gravity, per unit of length
Z = centre of gravity of cross section
M = torsional centre
a = distance between Z and M
L = 2l = length of span
f = maximum ordinate of the parabolic curve of the arch
b = width of bridge
F_b = area of cross section of arch
y = vertical deflection at distance x from origin
z = horizontal deflection at distance x from origin
ψ = angle of torsion with respect to axis of gravity at distance x from origin
$L_k = L\left(1+8\frac{f^2}{L^2}\right)$ = length of arch (approximately)
K = damping modulus
$\omega = \frac{\gamma b}{2v}$ is the "reduced frequency", in which
b = width of bridge
v = wind velocity
γ = circular frequency of wind-induced vibrations



Due to its much greater rigidity, this in comparison to suspension bridges, the 2nd-order theory is not applicable for a stiffened arch of the closed type.

The equations of motion are therefore as follows:

1. Purely vertical displacements:

$$EI_v\frac{\partial^4 y}{\partial x^4}+m\frac{\partial^2 y}{\partial t^2}+\frac{8f}{L^2}H_{(t)}=p(x,t)$$

while also is in force:

$$H_{(t)} \cdot \frac{L_k}{EF_b} = \frac{8f}{L^2} \int_0^L y\,dx$$

when the elongation of the vertical members is neglected.

2. The differential equations of simultaneous torsional and horizontal vibration:

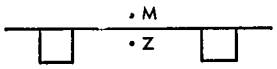
$$EC\frac{\partial^4 \psi}{\partial x^4} - GI_p \frac{\partial^2 \psi}{\partial x^2} + EI_h . a \frac{\partial^4 z}{\partial x^4} + \Theta \frac{\partial^2 \psi}{\partial t^2} + \frac{8fb}{L^2} H_{(t)} = q(x,t)$$

$$EI_h . a \frac{\partial^4 \psi}{\partial x^4} + EI_h \frac{\partial^4 z}{\partial x^4} + m \frac{\partial^2 z}{\partial t^2} = r(x,t)$$

while under the same conditions as those assumed above it is seen that:

$$H_{(t)} \frac{L_k}{EF_b} = \frac{4fb}{L^2} \int_0^L \psi\,dz$$

When is taken $p(x,t)=0$, $q(x,t)=0$ and $r(x,t)=0$ solution of the above equations will give the natural frequencies of the system.



We shall not go any further into this part of the problem, because the deductions would take up too much space and shall continue with the flutter problem itself.

Flutter equations have been drawn up for the 1st antimetric harmonic vibrations where $\int y\,dx = 0$, so that the flutter vibrations do not give rise to any change in the force in the arch. Simpler equations are the result. In addition, the effect of GI_p, which is very small in proportion to EC, is ignored. If desired, an approximation thereof can be taken into account by increasing EC with the correct proportion.

Under these conditions and taking into account the damping influence of the structure, the flutter equations are:

$$\left.\begin{aligned} &EI_v \frac{\partial^4 y}{\partial x^4} + KI_v \frac{\partial^5 y}{\partial x^4 \partial t} + m \frac{\partial^2 y}{\partial t^2} = P(x,t) \\ &EC\frac{\partial^4 \psi}{\partial x^4} + KC \frac{\partial^5 \psi}{\partial x^4 \partial t} + EI_h . a \frac{\partial^4 z}{\partial x^4} + KI_h . a \frac{\partial^5 z}{\partial x^4 \partial t} + \Theta \frac{\partial^2 \psi}{\partial t^2} = Q(x,t) \\ &EI_h . a \frac{\partial^4 \psi}{\partial t^4} + KI_h . a \frac{\partial^5 \psi}{\partial x^4 \partial t} + EI_h \frac{\partial^4 z}{\partial t^4} + KI_h \frac{\partial^5 z}{\partial x^4 \partial t} + m \frac{\partial^2 z}{\partial t^2} = R(x,t) \end{aligned}\right\} \quad \text{(I}^a\text{)}$$

P(x, t); Q(x, t) and R(x, t) are the wind loadings.

According to the publications that have appeared to date, they are:

$$P(x,t)=P_0+A_1\psi-B_1\frac{\partial\psi}{\partial t}+C_1y-D_1\frac{\partial y}{\partial t}$$

$$Q(x,t)=Q_0+A_2\psi-B_2\frac{\partial\psi}{\partial t}+C_2y-D_2\frac{\partial y}{\partial t}+E_2z-F_2\frac{\partial z}{\partial t} \qquad \text{(I}^b\text{)}$$

$$R(x,t)=R_0+A_3\psi-B_3\frac{\partial\psi}{\partial t}+C_3y-D_3\frac{\partial y}{\partial t}+E_3z-F_3\frac{\partial z}{\partial t}$$

The terms P_0, Q_0 and R_0, which are constant, occasion static deflections and may be ignored in subsequent deductions.

The quantities A_1, B_1..... E_3 and F_3 can be obtained from wind measurements. The former are seen to be functions of what is known as the reduced frequency $\frac{\gamma b}{2v}=\omega$. Accordingly, these quantities can be regarded as constants if the reduced frequency is given a certain value.

The equations can be solved by means of the following subsitutions:

$$y=\Sigma\,\Phi_{kx}.f(t)$$
$$\psi=\Sigma\frac{2}{b}\,\Phi_{kx}.\varphi(t) \qquad \text{(I}^c\text{)}$$
$$z=\Sigma\,\Phi_{kx}.g(t)$$

The quantities C_1, A_2, A_3, C_3, D_3, E_2 and E_3 are also seen to be negligible.

Introduction of the substitutions produce the following simultaneous differential equations:

$$f''(t)+2n_v.f'(t)+p_v^2.f(t)+2\overline{n}_v.\varphi'(t)-\overline{p}_v^2.\varphi(t)=0$$
$$\varphi''(t)+2n_w\varphi'(t)+p_w^2.\varphi(t)+2n_{wh}.g'(t)+p_{wh}^2g(t)+2\overline{n}_w.f'(t)-\overline{p}_w^2f(t)=0 \qquad \text{(II}^a\text{)}$$
$$g''(t)+2n_h.g'(t)+p_h^2.g(t)+2n_{hw}.\varphi'(t)+p_{hw}^2.\varphi(t)=0$$

In which:

$$2n_v=\frac{k^4\pi^4KI_v}{ml^4}+\frac{D_1}{m} \qquad 2\overline{n}_v=\frac{2B_1}{bm}$$

$$p_v^2=\frac{k^4\pi^4EI_v}{ml^4} \qquad \overline{p}_v^2=\frac{2A_1}{bm}$$

$$2n_w=\frac{k^4\pi^4KC}{\theta l^4}+\frac{B_2}{\theta} \qquad 2n_{wh}=\frac{k^4\pi^4abKI_h}{2\theta l^4}+\frac{bF_2}{\theta}$$

$$p_w^2=\frac{k^4\pi^4EC}{\theta l^4} \qquad p_{wh}^2=\frac{k^4\pi^4abEI_h}{2\theta l^4}$$

$$2\overline{n}_w=\frac{bD_2}{2\theta} \qquad \overline{p}_w^2=\frac{bC_2}{2\theta} \qquad \text{(II}^b\text{)}$$

$$2n_h=\frac{k^4\pi^4KI_h}{ml^4}+\frac{F_3}{m} \qquad 2n_{hw}=\frac{2k^4\pi^4aKI_h}{bml^4}+\frac{2B_3}{m}$$

$$p_h^2=\frac{k^4\pi^4EI_h}{ml^4} \qquad p_{hw}^2=\frac{2k^4\pi^4aEI_h}{bml^4}$$

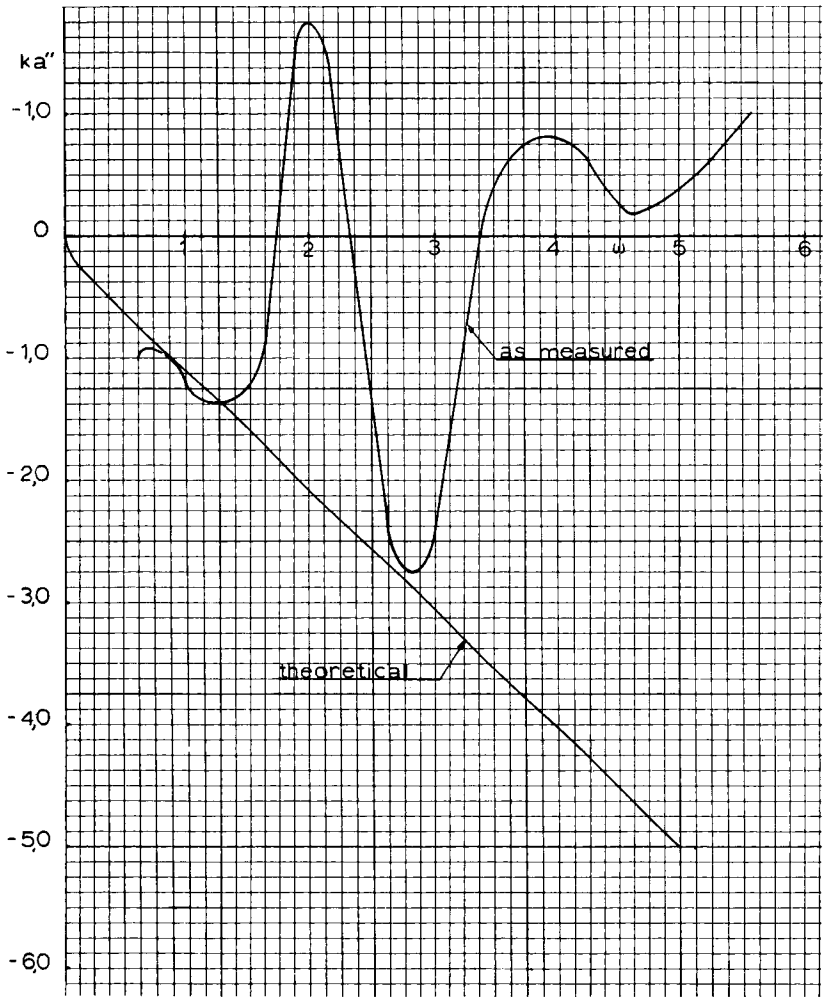
$$\Phi_{kx}=\left[(\cosh\lambda x-\cos\lambda x)-\frac{\cosh\lambda L-\cos\lambda L}{\sinh\lambda L-\sin\lambda L}(\sinh\lambda x-\sin\lambda x)\right]$$

to be used for the value $k\pi=\lambda L=2\frac{1}{2}\pi$ (approximately).

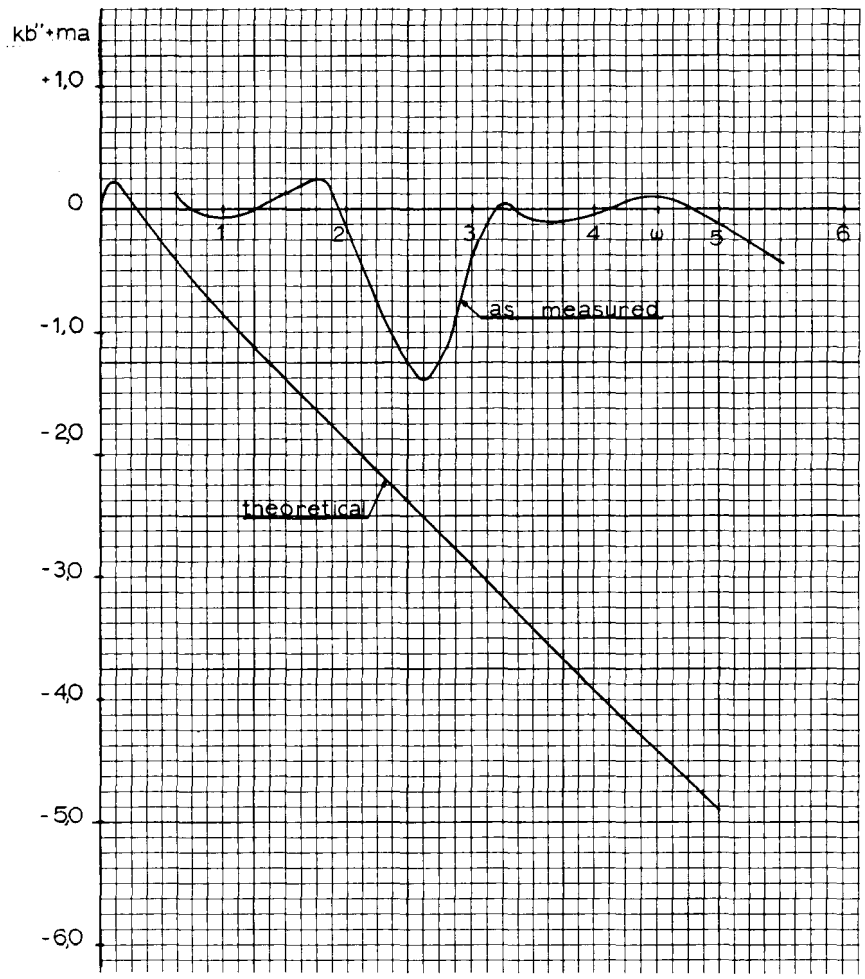
Solving the ordinary simultaneous differential equations (IIa) with the well known substitutions

$$\left.\begin{aligned} f(t)&=\Sigma C e^{rt}\\ \Phi(t)&=\Sigma \gamma_1 C e^{rt}\\ g(t)&=\Sigma \gamma_2 C e^{rt}\end{aligned}\right\} \quad \ldots\ldots\ldots\

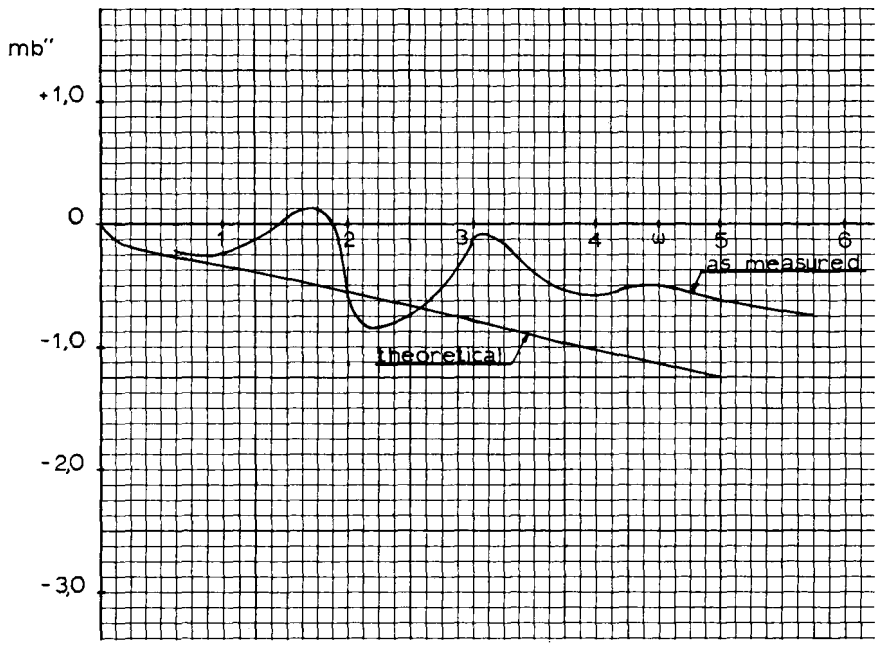
Relation between coefficient ka'' and the reduced frequency ω.



Relation between the coefficients $kb'' + ma''$ and the reduced frequency ω.



Relation between coefficient mb'' and the reduced frequency ω.



Appendix II The vibration absorber

The differential equations for this problem are:

$$EI_v\frac{\partial^4 y}{\partial x^4}+KI_v\frac{\partial^5 y}{\partial x^4\partial t}+m\frac{\partial^2 y}{\partial t^2}=p_0\sin\omega t$$

$$M_1\frac{d^2z}{dt^2}+K_1\frac{d(z-h)}{dt}+c_1(z-h)=0$$

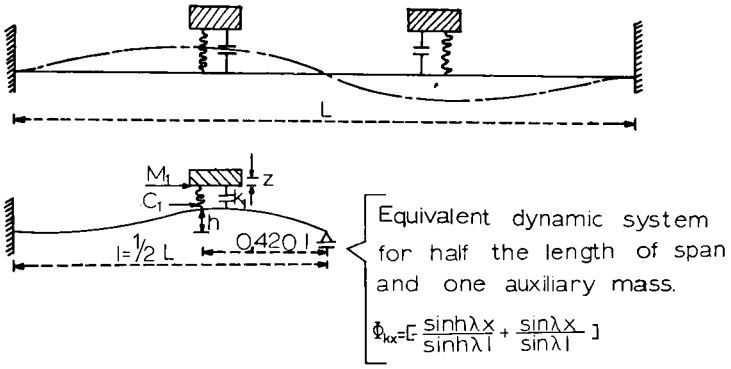


Figure II-1

in which h = deflection of the girder at position where spring and vortex-flow absorber are attached to the girder.

There are two ways of solving this set of equations.

1. By means of the assumption

$$y=f_1(x)\sin\omega t+f_2(x)\cos\omega t$$

in which the force exerted by the auxiliary mass M, i.e.

$$K_1\frac{d(z-h)}{dt}+c_1(z-h)=-M_1\frac{d^2z}{dt^2}$$

is applied in such a manner that a sudden change in the shearing-force diagram is produced at the point of application. This method is very cumbersome and produces a transcendent equation lacking in clarity. It has one advantage, however; it shows the exact deflection curve directly;

2. By using normal functions.

Since we are concerned with resonance at the lowest natural frequency, the effect of all the high harmonics is so small that it can be ignored. True, the deflection curve will not be mathematically exact, but it will be represented more or less exactly by the elastic line as a result of the lowest natural vibration.

Both the loading and the effect of the forces applied to the girder by the auxiliary mass are to be expanded in normal function series. The first equation will then have the following appearance, in which only half of the bridge's length is dealt with,

because the normal function for the entire structure can be divided up into two equal though antimetric branches.

$$E I_v \frac{\partial^4 y}{\partial x^4} + K I_v \frac{\partial^5 y}{\partial x^4 \partial t} + m \frac{\partial^2 y}{\partial t^2} = \Sigma - \frac{M_1}{\alpha_k l} \cdot \Phi_{ka} \cdot \Phi_{kx} \frac{d^2 z}{dt} + \Sigma \frac{p_o}{\alpha_k l} \cdot \bar{\Phi}_{ka} \Phi_{kx} \sin \omega t \quad \ldots\ldots\ldots (I)$$

In which:

$$\alpha_k l = \int_o^l \Phi_{kx}^2 \, dx \quad ; \quad \bar{\Phi}_{kx} = \int_o^l \Phi_{kx} \, dx$$

and:

$$\Phi_{ka} = \Phi_{kx}]_{x=a}$$

The load p_o is taken as being uniformly distributed.

Substituting $y = \bar{\Phi}_{kx} \cdot f(t)$ in (I) we get

$$f''(t) + 2q_k f'(t) + p_k^2 f(t) + \beta_k \frac{d^2 z}{dt^2} = \bar{p}_o \sin \omega t \quad \ldots\ldots\ldots\ldots\ldots\ldots\ldots\ldots\ldots (II)$$

in which:

$$p_k^2 = \frac{k^4 \pi^4 E I_v}{m l^4} \quad ; \quad 2q_k = \frac{k^4 \pi^4 K I_v}{m l^4}$$

$$\beta_k = \frac{M_1 \Phi_{ka}}{\alpha_k m l} = \frac{M_1}{M_o} \cdot \frac{\Phi_{ka}}{\alpha_k} \quad ; \quad \bar{p}_o = \frac{p_o \bar{\Phi}_{ka}}{\alpha_k m l} = \frac{p_o}{M_o} \cdot \frac{\bar{\Phi}_{ka}}{\alpha_k}$$

The 2nd equation is:

$$M_1 \frac{d^2 z}{dt^2} + K_1 \frac{dz}{dt} + C_1 z = K_1 \frac{dh}{dt} + C_1 h \quad \ldots\ldots\ldots\ldots\ldots\ldots\ldots\ldots\ldots (III^a)$$

In this equation:

$$h = \Phi_{ka} \cdot f(t) \quad \text{and therefore} \quad \frac{dh}{dt} = \Phi_{ka} \cdot f'(t) \quad \ldots\ldots\ldots\ldots\ldots\ldots (III^b)$$

(III^b) substituted in (III^a) gives:

$$\frac{d^2 z}{dt^2} + 2\eta_1 \frac{dz}{dt} + p_1^2 z = 2\bar{\eta}_1 f'(t) + \bar{p}_1^2 f(t) \quad \ldots\ldots\ldots\ldots\ldots\ldots\ldots\ldots (IV)$$

in which:

$$p_1^2 = \frac{C_1}{M_1} \; ; \; 2\eta_1 = \frac{K_1}{M_1} \; ; \; \bar{p}_1^2 = \frac{C_1 \Phi_{ka}}{M_1} \quad \text{and} \quad 2\bar{\eta}_1 = \frac{K_1 \Phi_{ka}}{M_1}$$

Eliminating z from equations (II) and (IV), we get the 4th order differential equation in f(t) reading

$$f''''(t) + A f'''(t) + B f''(t) + C f'(t) + D f(t) = \bar{p}_o \left[(p_1^2 - \omega^2) \sin \omega t + 2\eta \omega \cos \omega t \right] \quad \ldots\ldots\ldots\ldots (V)$$

in which:

$$A = 2\left\{q_k + (1 + \Phi_{ka} \cdot \beta_k)\, n_1\right\} \qquad B = p_k^2 + (1 + \Phi_{ka} \cdot \beta_k) p_1^2 + 4 q_k \cdot n_1$$

$$C = 2\left\{n_1 \cdot p_k^2 + q_k \cdot p_1^2\right\} \qquad D = p_k^2 \cdot p_1^2$$

The method of undetermined coefficients is used to calculate the forced vibration, the following equation being used for the purpose

$$f(t) = P \sin \omega t + Q \cos \omega t$$

By this method the forced vibration is found to be

$$y = \bar{p}_0 \cdot \frac{\sqrt{(p_1^2 - \omega^2)^2 + 4 n_1^2 \omega^2}}{\sqrt{(\omega^4 - B\omega^2 + D)^2 + (A\omega^3 - C\omega)^2}} \cdot \Phi_{kx} \sin(\omega t + \Theta_k) \quad \ldots\ldots\ldots\ldots\ldots\ldots \quad (V^a)$$

θ_K is the angle of phase-shift, which, however, is of little practical importance.
z is found to be

$$\frac{d^4 z}{dt^4} + A \frac{d^3 z}{dt^3} + B \frac{d^2 z}{dt^2} + C \frac{dz}{dt} + D z = \bar{p}_0 \left[\bar{p}_1^2 \sin \omega t + 2 \bar{n} \omega \cos \omega t\right] \quad \ldots\ldots\ldots\ldots \quad (VI)$$

and the forced vibration is then

$$z = \bar{p}_0 \cdot \frac{\sqrt{\bar{p}_1^4 + 4 \bar{n}_1^2 \omega^2}}{\sqrt{(\omega^4 - B\omega^2 + D)^2 + (A\omega^3 - C\omega)^2}} \cdot \Phi_{ka} \sin(\omega t + \Theta_k) \quad \ldots\ldots\ldots\ldots\ldots\ldots \quad (VI^a)$$

These are the expressions we find in the text-books on mechanical vibration; they are much clearer than the transcendent equations by the 1st method. The standard form Φ_{kx} for a half span is equal to:

$$\Phi_{kx} = \left[-\frac{\sinh \lambda x}{\sinh \lambda l} + \frac{\sin \lambda x}{\sin \lambda l}\right], \text{ also } \alpha_k = 1$$

After some trials a favourable combination was found with the following numerical values:

$p_k^2 = 15{,}374$; $\bar{p}_1^2 = 15{,}611$; $n_1 = 0{,}365$ and $\bar{n}_1 = 0{,}389$

giving:

$A = 0{,}787$; $B = 30{,}455$; $C = 11{,}747$ and $D = 224{,}937$.

Taking λ as equal to $\frac{\omega}{p_k}$, we get a dynamic amplification factor for x = a of

$$\varphi_1 = \frac{\sqrt{(0{,}952 - \lambda^2)^2 + 0{,}0346 \lambda^2}}{\sqrt{(\lambda^4 - 1{,}981 \lambda^2 + 0{,}952)^2 + (0{,}201 \lambda^2 - 0{,}195 \lambda)^2}}$$

for the bridge and

$$\varphi_2 = \frac{\sqrt{1{,}030 + 0{,}0394 \lambda^2}}{\sqrt{(\lambda^4 - 1{,}981 \lambda^2 + 0{,}952)^2 + (0{,}201 \lambda^3 - 0{,}195 \lambda)^2}}$$

for the auxiliary mass, while φ_0 is the dynamic amplification factor for the bridge without vibration absorber.

In tabular form the results obtained are:
See also Figure II-2.

λ	φ_0	φ_1	φ_2
0,6	1,56	1,60	2,55
0,7	1,96	2,06	4,15
0,8	2,78	3,21	8,95
0,9	5,26	7,53	33,13
1,0	109,60	6,48	32,75
1,1	4,76	5,85	17,28
1,2	2,27	2,59	4,72

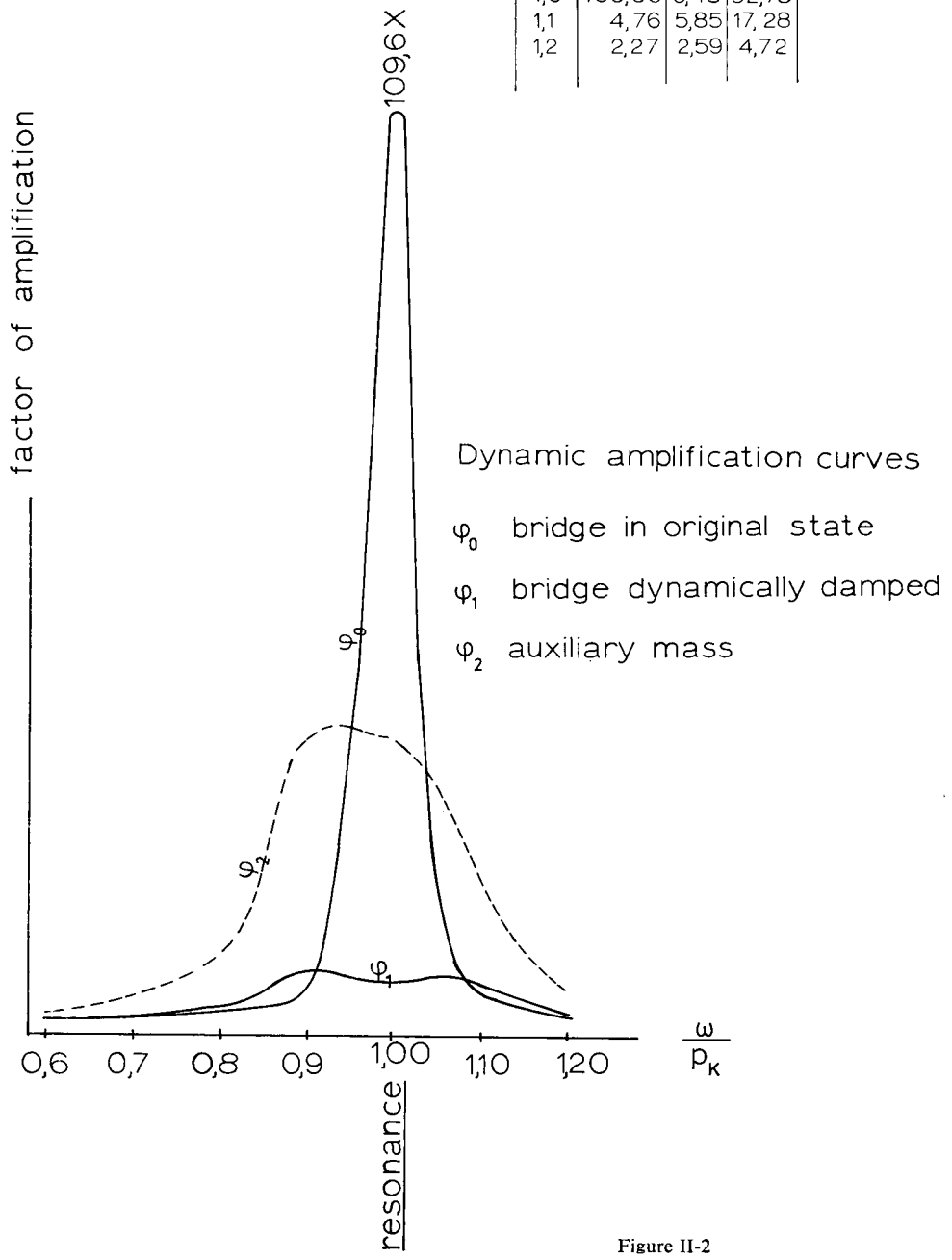


Figure II-2

Appendix III The orthotropic deck

For a straight bar supported arbitrarily and loaded by arbitrary forces of intensities $P_1, \ldots P_{n-1}, P_n, P_{n+1} \ldots$ (see Figure III-1) at points $1, \ldots n-1, n, n+1$, spaced at equal distances c from one another the following relation of finite differences is, as is commonly known, applicable.

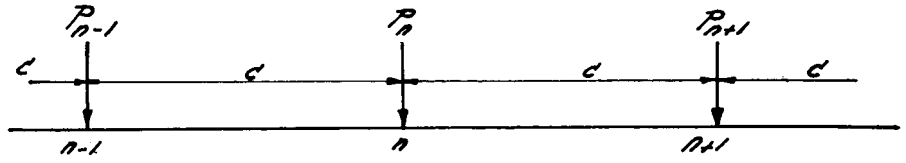


Figure III-1

$$\Delta^2 M_n = -c.P_n \quad \ldots\ldots\ldots\

$$\Delta^4 y_n = \frac{-c^2}{EI}\left[\frac{1}{6}\Delta^4 M_n + \Delta^2 M_n\right]$$

or substituting (I) and taking the second higher difference gives us

$$\Delta^4 y_n = \frac{c^3}{EI}\left[\frac{1}{6}\Delta^2 P_n + P_n\right]$$

In equations for plates the term y is usually replaced by w. So we get

$$\Delta^4 w_n = \frac{c^3}{EI_1}\left[\frac{1}{6}\Delta^2 P_n + P_n\right] \quad \ldots\ldots\ldots\ldots\ldots\ldots\ldots\ldots\ldots\ldots\ldots\ldots \text{(IV)}$$

Accordingly, I_1 represents the moment of inertia of the stringers welded on to the deck plate, i.e. of the profile as given in Figure III-3.

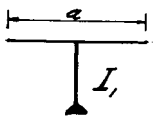
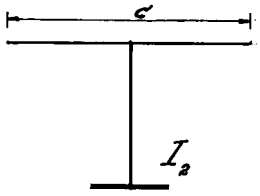


Figure III-3



c = distance c.o.c. of cross girders.

Figure III-4

If the stringers are attached at distance 'a' from one another and if I_2 is the moment of inertia of a cross girder (Figure III-4), the reaction P_n of cross girder on stringers will be the following (upwards negative):

$$P_n = -aEI_2 \cdot \frac{\partial^4 w_n}{\partial y^4}$$

therefore:

$$\Delta^2 P_n = -aEI_2 \cdot \Delta^2 \frac{\partial^4 w_n}{\partial y^4} \quad \text{in which:}$$

$$\Delta^2 \frac{\partial^4 w_n}{\partial y^4} = \frac{\partial^4 w_{n-1}}{\partial y^4} - 2\frac{\partial^4 w_n}{\partial y^4} + \frac{\partial^4 w_{n+1}}{\partial y^4}$$

Consequently, the partial difference differential equation for the torsion-free floor grillage system is

$$\frac{\Delta^4 w_n}{c^4} = -\frac{aEI_2}{cEI_1}\left[\frac{1}{6}\Delta^2 \frac{\partial^4 w_n}{\partial y^4} + \frac{\partial^4 w_n}{\partial y^4}\right] \quad \ldots\ldots\ldots\ldots\ldots\ldots\ldots\ldots\ldots\ldots \text{(V)}$$

This equation is used for this orthotropic system since it has a very slight torsional stiffness. The torsional rigidity can be included later in quite a simple manner, though not with complete accuracy from a theoretical point of view. Since the influence is very small itself, the result obtained in such a way is sufficiently correct.

A solution to (V) can be obtained with the assumption

$$w_n = \Sigma X_n \cdot \phi_{yk} \quad \ldots\ldots\ldots\ldots\ldots\ldots\ldots\ldots\ldots\ldots\ldots\ldots\ldots\ldots \text{(VI}^a\text{)}$$

in which Φ_{yk} represents an arbitrary normal function with arbitrary boundary conditions along the Y axis. If b represents the length of span along the Y axis, we see that

$$\Delta^4 w_n = \Sigma \Delta^4 X_n \cdot \phi_{yk} \qquad \text{and} \qquad \frac{\partial^4 w_n}{\partial y^4} = \Sigma \frac{k^4 \pi^4}{b^4} \cdot X_n \cdot \phi_{yk} \quad \ldots\ldots\ldots\ldots\ldots\ldots (VI^b)$$

Substitution of (VI[a]) and (VI[b]) in (V) and elimination of Φ_{yk} gives us

$$\Delta^4 X_n = -\frac{k^4 \pi^4 c^4}{b^4} \cdot \frac{a E I_2}{c E I_1} \left[\frac{1}{6} \Delta^2 X_n + X_n\right]$$

Let $\frac{k^4 \pi^4 a E I_2}{b^4} = \alpha$ then

$$\Delta^4 X_n = -\frac{\alpha c^3}{6 E I_1} \left[\Delta^2 X_n + 6 X_n\right] \quad \ldots\ldots\ldots\ldots\ldots\ldots\ldots\ldots\ldots\ldots\ldots\ldots\ldots\ldots\ldots\ldots (VII)$$

Introduce further $\frac{\alpha c^3}{6 E I_1} = \omega$

The general solution for this type of linear difference equations is

$$X_n = \Sigma C \varepsilon^n$$

giving

$$\Delta^2 X_n = \Sigma C \mu \varepsilon^n$$

and

$$\Delta^4 X_n = \Sigma C \mu^2 \varepsilon^n$$

in which

$$\mu = \frac{(\varepsilon - 1)^2}{\varepsilon}$$

Substitution in equation VII gives the characteristic equation

$$\mu^2 = -\omega(\mu + 6) \quad \ldots\ldots\ldots\ldots\ldots\ldots\ldots\ldots\ldots\ldots\ldots\ldots\ldots\ldots\ldots\ldots\ldots\ldots\ldots\ldots (VII^a)$$

Since ω is a known quantity, we can determine μ, after which we can calculate the four ε values from

$$\mu = \frac{(\varepsilon - 1)^2}{\varepsilon} \qquad \text{or} \qquad \varepsilon^2 - (2 + \mu)\varepsilon + 1 = 0 \quad \ldots\ldots\ldots\ldots\ldots\ldots\ldots\ldots\ldots\ldots (VII^b)$$

Indicating the roots by $\varepsilon_1, \varepsilon_2, \varepsilon_3$ and ε_4 we see that according to (VII[b])

$$\varepsilon_1 \cdot \varepsilon_2 = 1 \qquad \text{and} \qquad \varepsilon_3 \cdot \varepsilon_4 = 1$$

The roots nearly always emerge in a complex form, so that written in trigonometrical form we get

$$\varepsilon_1 = e^{\delta}(\cos\varphi + i \sin\varphi) \qquad \varepsilon_3 = e^{\delta}(\cos\varphi - i \sin\varphi)$$

$$\varepsilon_2 = e^{-\delta}(\cos\varphi - i \sin\varphi) \qquad \varepsilon_4 = e^{-\delta}(\cos\varphi + i \sin\varphi)$$

From above:

$$\mu=\frac{(\varepsilon-1)^2}{\varepsilon}=\varepsilon-2+\frac{1}{\varepsilon}$$

therefore:

$$\mu_1=\varepsilon_1-2+\frac{1}{\varepsilon_1}=2\left[\cosh\delta\cos\varphi+i\sinh\delta\sin\varphi-1\right]$$

$$\mu_2=\varepsilon_3-2+\frac{1}{\varepsilon_3}=2\left[\cosh\delta\cos\varphi-i\sinh\delta\sin\varphi-1\right]$$

with which:

$$\mu_1+\mu_2=4\cosh\delta\cos\varphi-4$$

$$\mu_1\mu_2=4(\cosh\delta-\cos\varphi)^2$$

The characteristic equation for μ is:

$$\mu^2+\omega\mu+6\omega=0 \quad \text{therefore:}$$

$$4\cosh\delta\cos\varphi-4=-\omega \quad \text{and} \quad 4(\cosh\delta-\cos\varphi)^2=6\omega$$

from which the solution:

$$\cos\varphi=\frac{1}{4}\left[-\sqrt{6\omega}+\sqrt{2\omega+16}\right]$$

$$\cosh\delta=\frac{1}{4}\left[+\sqrt{6\omega}+\sqrt{2\omega+16}\right]$$

The solution of each harmonic then emerges in the following real form:

$$w_n=\left[e^{-\delta n}\left\{\bar{A}\cos n\varphi+\bar{B}\sin n\varphi\right\}+e^{+\delta n}\left\{\bar{C}\cos n\varphi+\bar{D}\sin n\varphi\right\}\right]\Phi_{yk}$$

Since the orthotropic deck plate sections possess asymmetrical boundary conditions, which makes calculation of the natural function Φ_{yk} a lengthy matter, we would give a simpler example here, namely

for $y = 0$ and $y = b$ then $\Phi_{yk} = 0$ and $\dfrac{d\Phi_{yk}}{dy} = 0$.

In this case

$$\Phi_{yk}=\left[(\cosh\lambda y-\cos\lambda y)-\frac{\cosh\lambda b-\cos\lambda b}{\sinh\lambda b-\sin\lambda b}(\sinh\lambda y-\sin\lambda y)\right] \quad \ldots\ldots\ldots\ldots \text{(VII}^c\text{)}$$

the consecutive roots of the frequency equation being $k\pi = \lambda b = 4.730;\ 10.996;\ 17.279\ldots\ldots$ The normal function given in (VII^c) has been normalized to

$$\int_0^b \Phi_{yk}^2\,dy=1$$

The deck is regarded as being very long in the direction of the x axis, which makes the integration constants C and D = 0. So we get

$$w_n=e^{-\delta n}\left[\bar{A}\cos n\varphi+\bar{B}\sin n\varphi\right]\Phi_{yk}$$

$$\frac{\partial^4 w_n}{\partial y^4}=e^{-\delta n}\left[\bar{A}\cos n\varphi+\bar{B}\sin n\varphi\right]\frac{\partial^4\Phi_{yk}}{\partial y^4}$$

Since $\frac{\partial^4 \Phi_{yk}}{\partial y^4} = \lambda^4 \Phi_{yk}$ we get

$$\frac{\partial^4 w_n}{\partial y^4} = \lambda^4 w_n = \frac{k^4 \pi^4}{b^4} w_n = \frac{\alpha}{aEI_2} w_n$$

Furthermore

$$P_n = aEI_2 \frac{\partial^4 w_n}{\partial y^4} = \alpha w_n$$

(P_n is in this case the force, as a result of the stringers, acting on the cross girders)

Using equation I we arrive at the equation

$$w_n = -\frac{1}{\alpha c} \Delta^2 M_n \quad \ldots\ldots\ldots\

The scale of reading is $\frac{1}{\overline{\Psi}_o}$ when

$$\overline{\Psi}_o = 2\left[\frac{w_n|_{n=0} - w_n|_{n=1}}{c} + \frac{c}{6EI_1}\left\{2M_n|_{n=0} + M_n|_{n=1}\right\}\right]\frac{1}{\Phi_{yk}}$$

On working this out we get

$$\overline{\Psi}_o = \frac{4(\cosh\delta - \cos\varphi)}{\alpha c^2 \cosh\delta}\cdot\left[1 + e^{-\delta n}(\sinh\delta - \cos\varphi) + \frac{\alpha c^3}{12EI_1}\cdot\frac{2\cosh\delta + \cos\varphi}{\cosh\delta - \cos\varphi}\right]$$

The ordinates of the influence line for the deflection $\mathfrak{M}_n$ at points $n = 0; 1; \ldots$ for each branch (the influence line is symmetrical) for each harmonic k are found to be

$$\mathfrak{M}_n = \frac{c.e^{-\delta n}\left[\cos n\varphi - \frac{\sinh\delta}{\sin\varphi}\cdot\sin n\varphi\right]\cdot\Phi_{yk}}{2\left[1 + e^{-\delta}(\sinh\delta - \cos\varphi) + \frac{\alpha c^3}{12EI_1}\cdot\frac{2\cosh\delta + \cos\varphi}{\cosh\delta - \cos\varphi}\right]} \quad \ldots\ldots\ldots\ldots\ldots\ldots\ldots\ldots \text{(VIII)}$$

The values of $\mathfrak{M}_n$ calculated by means of (VIII) only apply to points $n=0; 1; \ldots$ For intermediate values the various branches of the deflection line must be calculated by using the values of M_n and w_n at the same points ($n = 0; 1; \ldots$) and dividing then by $\overline{\Psi}_o$.

Using the higher harmonics of the normal function Φ_{yk} the solutions of the characteristic equations may not appear in complex form but emerge as real quantities. The equations for M_n and w_n are then

$$M_n = \left[C_1\varepsilon_1^n + C_3\varepsilon_3^n\right]\cdot\Phi_{yk}$$

and $\alpha c.w_n = -\left[C_1\mu_1\varepsilon_1^n + C_3\mu_2\varepsilon_3^n\right]\cdot\Phi_{yk}$, in which μ_1, μ_2, ε_1 and ε_3 can be determined by means of the characteristic equation. Applying the same boundary conditions we also find that

$$C_1 = \frac{\mu_2 + 2(1-\varepsilon_3)}{(\mu_2 - \mu_1) + 2(\varepsilon_1 - \varepsilon_3)} \qquad C_3 = -\frac{\mu_1 + 2(1-\varepsilon_1)}{(\mu_2 - \mu_1) + 2(\varepsilon_1 - \varepsilon_3)}$$

The remaining part is completely analogous to the theory for the complex solution expounded above. It is usually quite enough to take only the 1st harmonic into account and to calculate the longitudinal girders where Φ_{yk} is at its maximum. Accordingly, the real solutions are only considered if an influence plane of great accuracy is desired, which is superfluous as a rule.

If the influence line for the bending moment at the support is known, the influence line for any point of the span can be calculated from this influence line.

Needless to say, when applying the foregoing theory, the live loads have to be expanded in the same normal functions series.

The most unfavourably loaded longitudinal girders are those situated in the middle of the cross girders. For them the 1st harmonic, or at most the 1st and 3rd harmonics, can be regarded as quite accurate enough.

Inclusion of the effect of the torsional rigidity can be attempted in the following

manner. All the ordinates of the deflection plane calculated for a certain loading of the orthotropic plate are multiplied by the same factor $\rho < 1$ (to be calculated later). Between successive cross girders the torsional change in angle φ – thus also the horizontal displacements 'r' of the small longitudinal girders – can be determined from the deflection plane reduced to the factor ρ (see Figure III-5). The torsional moments acting on the respective cross girders can then be calculated from these angular deformations. For example, if we consider the heaviest-loaded cross girders simply supported at the ends, we get the condition illustrated in Figure III-6.

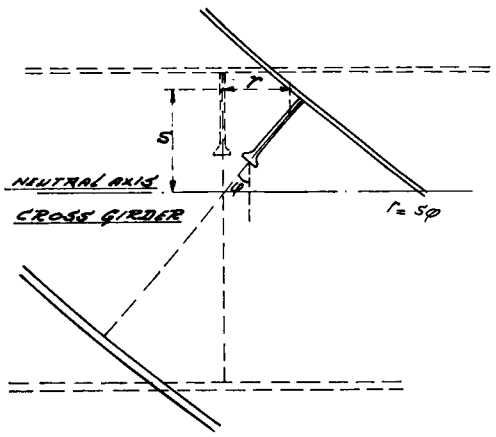


Figure III-5a

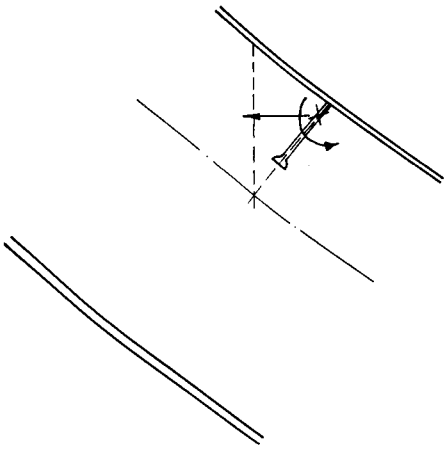


Figure III-5b

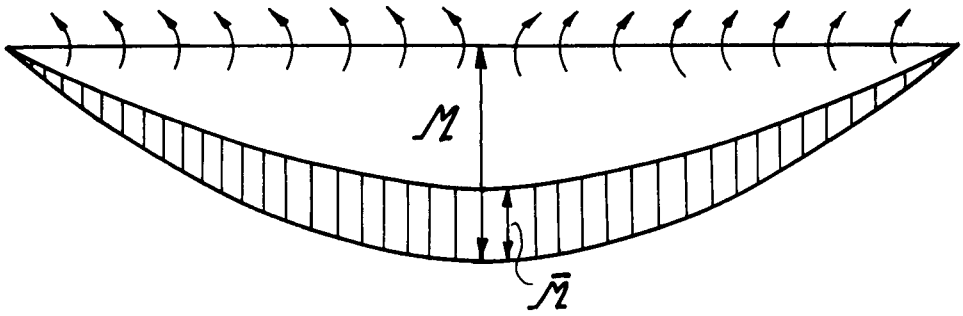


Figure III-6

The small torsional moments reduce the moment area to the extent shown by the shaded portion. The reduced deflection at the point of maximum bending can then be calculated and an equation obtained to determine the factor ρ. A similar reasoning can be adopted for the small longitudinal girders.

The bulb section is subject to an angular movement φ and the centres of gravity of the stringers receive a displacement 'r' in relation to their unbent state. The angles φ for the same bulb section between two successive cross girders are not constant.

Take the simple case of a girder freely supported along its edges, that means $\Phi_{yk} = \sin \frac{k\pi y}{b}$. Imagine that the cross girder bearing the heaviest load gives the following deflection line: $w = w_0 \sin \frac{\pi y}{b}$ and the two adjoining girders have the line $w = w_1 \sin \frac{\pi y}{b}$.

Reducing these values, we get

$$\left.\begin{aligned} w &= \rho w_0 \sin \frac{\pi y}{b} \\ w^1 &= \rho w_1 \sin \frac{\pi y}{b} \end{aligned}\right\} w_0 \rangle w_1$$

therefore: $\frac{dw}{dy} = \frac{\rho\pi}{b} w_0 \cos \frac{\pi y}{b}$ and $\frac{dw^1}{dy} = \frac{\rho\pi}{b} w_1 \cos \frac{\pi y}{b}$

giving: $\varphi = \frac{\rho\pi}{b}(w_0 - w_1)\cos \frac{\pi y}{b}$

The purely torsional moment of the stringer acting over a length dy of the cross girder is

$$dm_t = \frac{GI_p \varphi dy}{ac} = \frac{GI_p}{ac} \cdot \frac{\rho\pi}{b}(w_0 - w_1)\cos \frac{\pi y}{b} dy$$

Integrating for $y = 0 \rightarrow \frac{1}{2}b$ we find

$$\overline{M}_t = \int dm_t = \frac{\rho GI_p}{ac} \cdot (w_0 - w_1) \int_0^{\frac{1}{2}b} \cos \frac{\pi y}{b} d\frac{\pi y}{b} = \frac{\rho GI_p}{ac}(w_0 - w_1)$$

in which:

a = distance between the stringers,
c = distance between the cross girders,
b = length of the cross girders,
GI_p = torsional rigidity of the stringer.

The deflection curve along the x axis is fairly accurately represented bv

$$w = w_0 e^{-\alpha x} \cos \alpha x$$

from which α can be determined from the condition that

$$w_1 = w_0 e^{-\alpha x} \cos \alpha c$$

The reduced deflection diagram is expressed by the equation

$$w = \rho w_0 e^{-\alpha x} \cos \alpha x . \sin \frac{\pi y}{b}$$

therefore: $\varphi = \frac{\partial w}{\partial y} = \frac{\rho\pi}{b} w_0 e^{-\alpha x} \cos \alpha x \cdot \cos \frac{\pi y}{b}$, with which:

$$r = s\varphi = \frac{\rho\pi s}{b} w_0 e^{-\alpha x} \cos \alpha x . \cos \frac{\pi y}{b}$$

The resistance $dq=\frac{EI_h}{a}\cdot\frac{\partial^4 r}{\partial x^4}$ therefore:

$$dq=-\frac{\rho\pi sEI_h w_0}{ab}\cdot 4\alpha^4 e^{-\alpha x}\cos\alpha x\cos\frac{\pi y}{b}$$

The reaction on the central cross girder is

$$2\int_0^{\frac{1}{2}c} dq=-\frac{8\rho\pi sEI_h\alpha^4 w_0}{ab}\cdot\cos\frac{\pi y}{b}\int_0^{\frac{1}{2}c} e^{-\alpha x}\cos\alpha x\,dx=$$

$$=-\frac{4\rho\pi sEI_h\alpha^3 w_0}{ab}\cdot e^{-\frac{\alpha c}{2}}\left(\cos\frac{\alpha c}{2}+\sin\frac{\alpha c}{2}\right)\cos\frac{\pi y}{b}$$

which, partially integrated to y from $0\rightarrow\frac{1}{2}b$, gives

$$-\overline{M}=-\frac{4\rho s^2 EI_h\alpha^3 w_0}{a}\cdot e^{-\frac{\alpha c}{2}}\left(\cos\frac{\alpha c}{2}+\sin\frac{\alpha c}{2}\right)$$

Accordingly, the total relieving effect on the cross girder bearing the heaviest load for $x = 0$ and $y = \frac{1}{2}b$ is

$$-\overline{M}_{tot.}=\rho\left[\frac{GI_p}{ac}(w_0-w_1)+\frac{4s^2EI_h\alpha^3}{a}\cdot e^{-\frac{\alpha c}{2}}\left(\cos\frac{\alpha c}{2}+\sin\frac{\alpha c}{2}\right)w_0\right]$$

With this, the reduction in deflection is also known as a function of ρ.
ρ can be solved from the condition.

$$W_{original} - W_{reduction} = \rho \cdot W.$$

Appendix IV The primary longitudinal and cross girder system (theory)

List of notations

EI_l = flexural rigidity of the continuous longitudinal girder
EI_d = flexural rigidity of the cross girders
GI_p = torsional rigidity of the main girders to which each end of the cross girder is rigidly attached
c = distance c.o.c. of cross girders
b = width of bridge = length of cross girders
n = number indicating junction between longitudinal and cross girder or junction between main girder and cross girder (starting at 0)
P_n = force exerted by longitudinal girder on cross girder at point n
M_n = bending moment in longitudinal girder at point n
$\mathfrak{M}_n$ = torsional moment in main girder between points n – 1 and n
$\overline{m}_n = -(\mathfrak{M}_{n+1} - \mathfrak{M}_n)$ = bending moment at either end of the cross girder at point n caused by the torsional rigidity of the main girder
δn = deflection of n^{th} junction between longitudinal and cross girder
φn = angle of rotation at either end of n^{th} cross girder

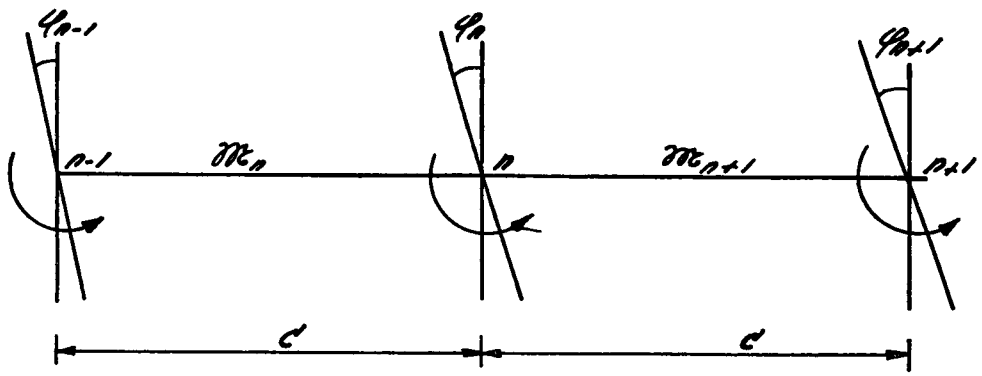


Figure IV-1

Let $\mathfrak{M}_n$ be the torsional moment in the n^{th} section of the box-shaped main girder and $\mathfrak{M}_{n+1}$ the torsional moment in the $n+1^{th}$ section, etc.

Let φ_n be the angle of rotation of the cross girder at the connection n of cross girder to box-shaped main girder, etc. The following then applies:

$$\varphi_n - \varphi_{n-1} = \frac{\mathfrak{M}_n \cdot c}{GI_p} \quad \text{and} \quad \varphi_{n+1} - \varphi_n = \frac{\mathfrak{M}_{n+1} \cdot c}{GI_p}$$

therefore:

$$\Delta^2 \varphi_n = \frac{c}{GI_p}(\mathfrak{M}_{n+1} - \mathfrak{M}_n) = -\frac{c}{GI_p}\overline{m}_n \quad \ldots\ldots\ldots\

The moment diagram for cross girder n on which force P_n exerted by the longitudinal girder acts is therefore as shown in Figure IV-2.

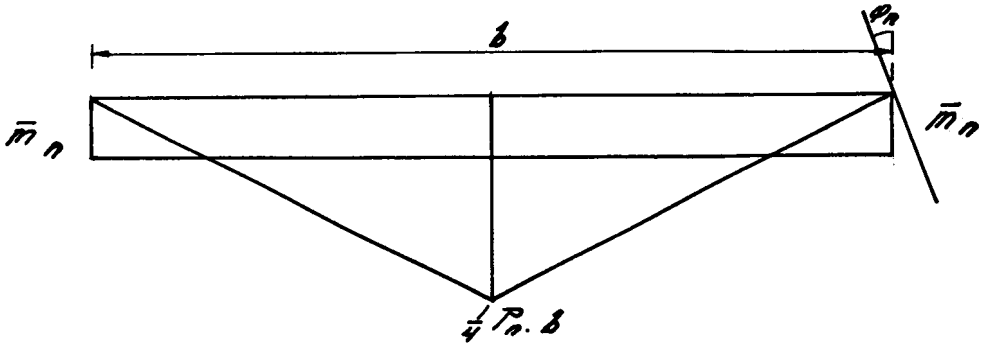


Figure IV-2

We get:

$$\varphi_n = \frac{b^2}{16 E I_d} P_n - \frac{b}{2 E I_d} \cdot \bar{m}_n$$

therefore:

$$\bar{m}_n = \frac{1}{8} b P_n - \frac{2 E I_d}{b} \varphi_n \quad \ldots\ldots\ldots\

Moreover is:

$$\delta_n = \frac{b^3}{192EI_d} P_n + \frac{1}{4} b\varphi_n = -\frac{b^3}{192cEI_d} \Delta^2 M_n + \frac{1}{4} b\varphi_n$$

With $t = \frac{b^3}{192EI_d}$ we get:

$$t.\Delta^2 M_n + c.\delta_n = \frac{1}{4} bc.\varphi_n \quad \ldots\ldots\ldots\

$$
\left.
\begin{aligned}
M_n &= C_1 e^{-\gamma n} + e^{-\lambda n}\left[C_2 \cos n\varepsilon + C_3 \sin n\varepsilon\right] \\
\delta_n &= \Phi_0 C_1 e^{-\gamma n} + \left[\Phi_1 C_2 + \Theta_1 C_3\right] e^{-\lambda n} \cos n\varepsilon + \left[-\Theta_1 C_2 + \Phi_1 C_3\right] e^{-\lambda n} \sin n\varepsilon \\
\varphi_n &= \Theta_0 C_1 e^{-\gamma n} + \left[\Phi_2 C_2 + \Theta_2 C_3\right] e^{-\lambda n} \cos n\varepsilon + \left[-\Theta_2 C_2 + \Phi_2 C_3\right] e^{-\lambda n} \sin n\varepsilon
\end{aligned}
\right\} \quad \text{(VI)}
$$

In these equations γ, λ and ε are numerical values obtained from the characteristic equation. Moreover:

$$
\left.
\begin{aligned}
\Phi_0 &= \frac{6+\mu_1}{\mu_1 s} & \Theta_0 &= \frac{\mu_1 r}{\mu_1 - a^2} \\
\Phi_1 &= \frac{\left[a_0^2 + b_0^2 + 6a_0\right]}{s\left[a_0^2 + b_0^2\right]} & \Theta_1 &= \frac{6 b_0}{s\left[a_0^2 + b_0^2\right]} \\
\Phi_2 &= \frac{r\left[a_0^2 + b_0^2 - a^2 a_0\right]}{(a_0 - a^2)^2 + b_0^2} & \Theta_2 &= \frac{a^2 b_0 r}{(a_0 - a^2)^2 + b_0^2}
\end{aligned}
\right\} \quad \text{(VI}^a\text{)}
$$

In which:

$$a_0 = 2(\cosh\lambda \cos\varepsilon - 1)$$

$$b_0 = 2 \sinh\lambda \sin\varepsilon$$

The boundary conditions are

$$M_0 = 1$$

The longitudinal girder is cut through at the location of the cross girder 0 and subjected to two equal but opposite bending moments $M_0 = 1$. The deflection curve naturally exhibits two branches. The magnitude of the reaction of the longitudinal girder to cross girder 0 is

$$P_0 = 2\,\frac{M_0 - M_1}{c}$$

while the fixed end moment of the cross girder to the torsionally rigid main girder is $\overline{m}_0$.

So we see that

$$\delta_0 = 2\,\frac{(M_0 - M_1)}{c} \cdot \frac{b^3}{48 E I_d} - \overline{m}_0 \cdot \frac{b^2}{8 E I_d}$$

and

$$\varphi_0 = 2\,\frac{(M_0 - M_1)}{c} \cdot \frac{b^2}{16 E I_d} - \overline{m}_0 \cdot \frac{b^2}{2 E I_d}$$

while

$$\overline{m}_0 = 2\,\frac{G I_p}{c}(\varphi_0 - \varphi_1)$$

Therefore we get the following boundary conditions:

$$
\left.
\begin{aligned}
M_0 &= 1 \\
\delta_0 &= \frac{b^3}{24 c . E I_d}\left[M_0 - M_1\right] - \frac{b^2 . G I_p}{4 c . E I_d}\left[\varphi_0 - \varphi_1\right] \\
\varphi_0 &= \frac{b^2}{8 c . E I_d}\left[M_0 - M_1\right] - \frac{b . G I_p}{c . E I_d}\left[\varphi_0 - \varphi_1\right]
\end{aligned}
\right\} \quad \text{(VI}^b\text{)}
$$

Substitution of (VI) in (VI^b) gives us the three equations solving C_1, C_2 and C_3. The best way to do this is numerically. There is no point in expressing C_1, C_2 and C_3 as formulae. Since the constants are now known, we can calculate the influence line for M_0 by using (VI).

The influence line for the reaction P_0 of longitudinal girder to cross girder 0 and for the bending moments at any point of the span of the longitudinal girder can be determined in the usual simple manner from the influence line for M_0.

We need this influence line when designing the connection between the longitudinal girder and cross girder and when calculating the maximum shear stresses in the web of the longitudinal girder. It cannot be used, however, for calculating the maximum moment in the cross girders. A fresh influence line must be computed for that purpose from other boundary conditions. The cross girder, not the longitudinal one, must be cut through at the point of intersection 0 and two equal but opposite moments of unity applied.

We are not giving these calculations, but only reproduce the four influence lines calculated for the Van Brienenoord Bridge. The influence line for the maximum moment in the cross girder is seen to differ in shape from the influence line for the support.

Appendix V The main girder system statically indeterminate to the 17th degree

The main girders consist of an arch (top chord) of great flexural stiffness and a similar bottom chord rigidly attached to each other at either end together with diagonally-placed cables between them. Arch, bottom chord and diagonal cables form in principle a curved chord truss. This truss was adopted as the statically determinate main system of the structure while the internal moments at the junctions in arch and bottom chord were selected as the redundants. An addition of the number of the junctions realizes that there are seventeen statically indeterminates.

The procedure is as follows. Two equal but opposite moments, each equal to unity, are in turn applied at each of the junctions after which all the deformations in the truss are calculated, i.e. the angular deviations at all the junctions and the deflection curve of the bottom chord. Figure V-1 shows this for two equal but opposite moments in junction No. 3 in the bottom chord. One moment acts upon section 3-2 and the other in the opposite direction on section 3-4. It is easy to understand that there are no reactions at the supports under these conditions. Accordingly, most of the members of the truss remain free of stress, except

horizontal girder sections 2-3 and 3-4;
arch sections III-IV and
diagonals 2-III, III-3; 3-IV and IV-4.

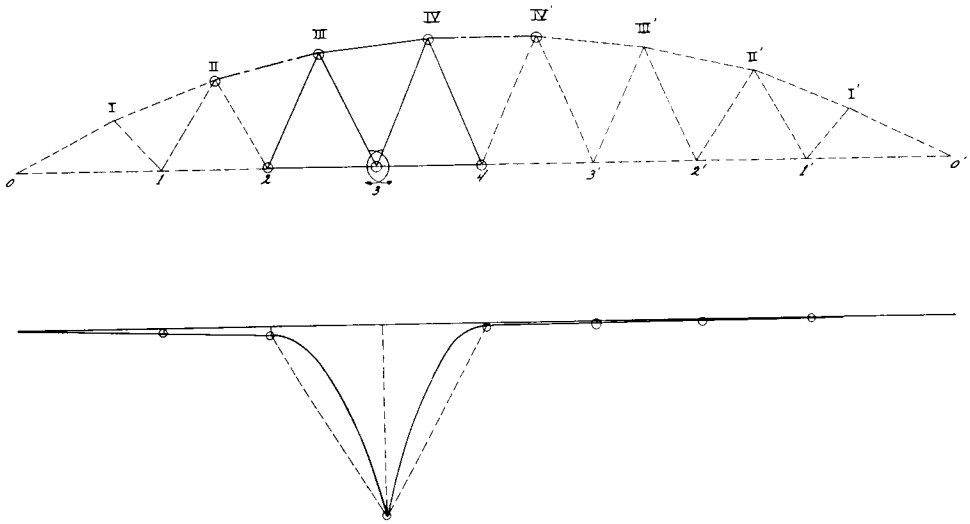
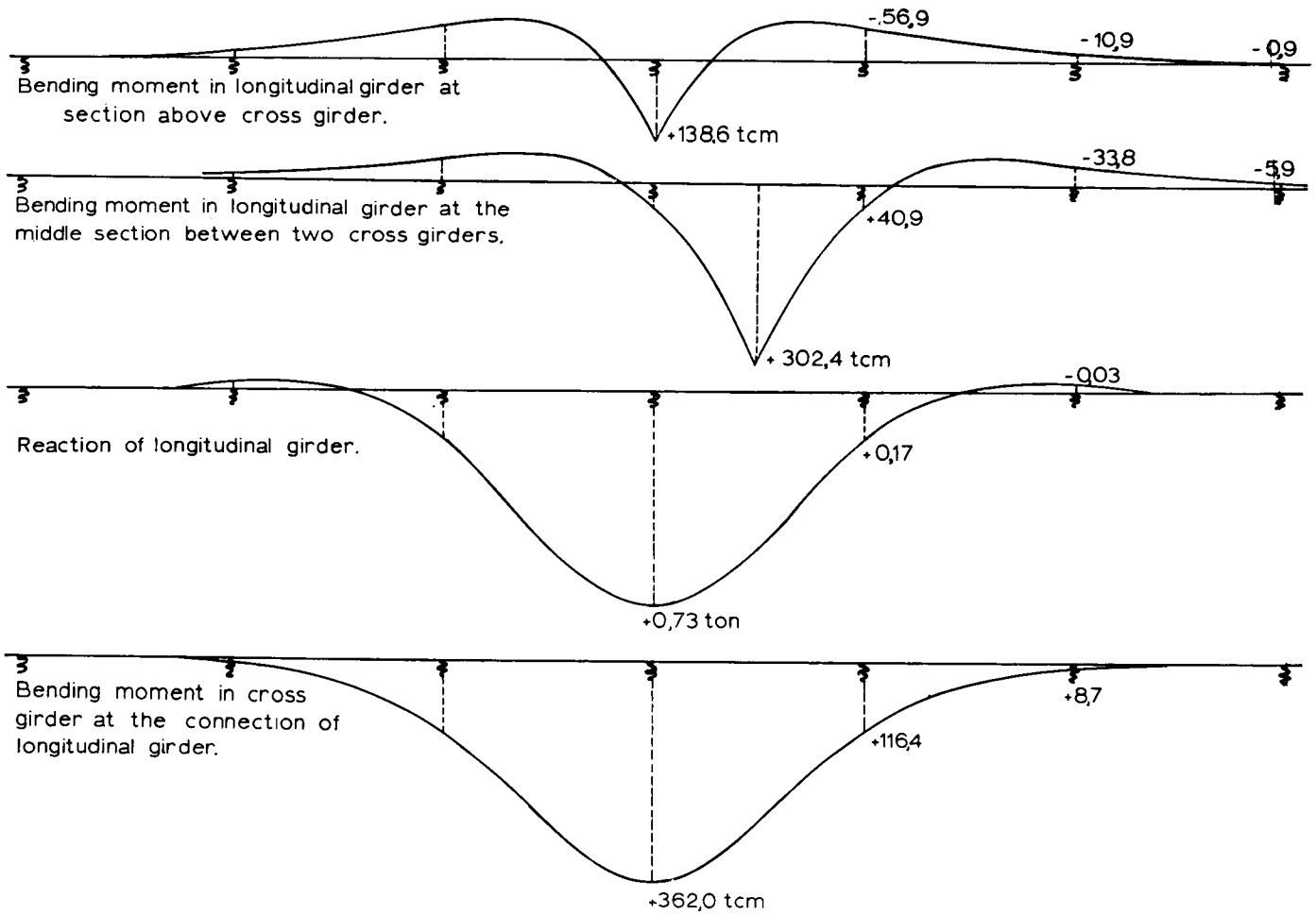


Figure V-1

Accordingly, it is also easy to understand that angular deviations occur in junctions 2, 3 and 4 in the bottom chord and in junctions II, III, IV and IV′ in the arch.

No angular deviations occur in any of the other junctions. Figure V-1 shows the deformation of the bottom chord; it is easy to understand that the members 0-1-2 and 4-3′-2′-1′-0′ do twist but remain straight. However, sagging does occur at those

Influence Lines



junctions. Point 3 sags considerably and the members 2-3 and 3-4 are bent as a result of the two moments applied at point 3. Consequently, Figure V-1 represents the entire deformation of the bottom chord for the loading conditions under consideration.

Figure V-2 shows the deformation for the case when two equal but opposite moments are acting in junction III of the arch, one moment acting upon arch section III-II and the other upon III-IV. So for the same reasons there will be angular deviations at arch junctions II, III and IV and in the bottom chord at junctions 1, 2, 3 and 4.

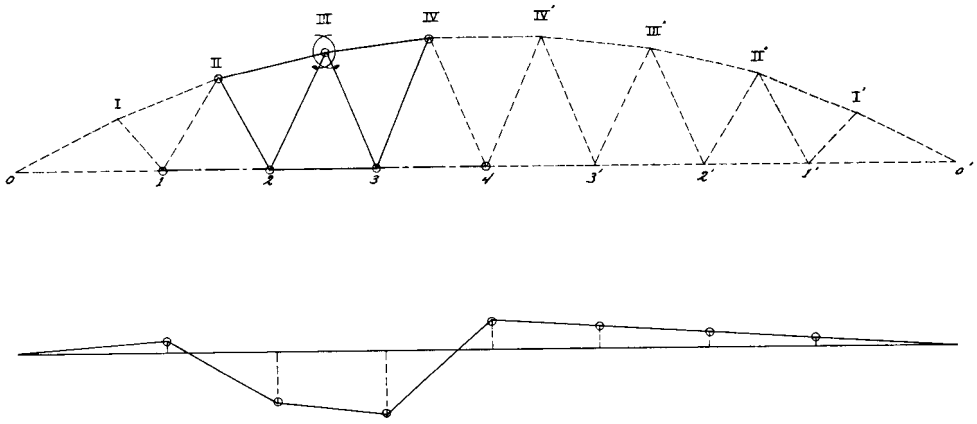


Figure V-2

Figure V-2 shows the deflection curve of the bottom chord. Since there are no moments acting in the bottom chord, the deflection consists of a broken series of lines, the individual lines being straight for each member. Accordingly, the members 4-3′-2′-1′-0′ are also straight. All the junctions are treated in the same manner, and only half of them need to be computed, because the truss is symmetrical. The calculated angle deviations are combined in a deformation square matrix, which contains many zeros, since the angle deviations usually manifest themselves at seven junctions only.

If the various columns of the square matrix are computed independently of each other, Maxwell's law of reciprocity affords an excellent check on possible mistakes in calculation.

This has been done for the bridge. The accuracy obtained was up to six places of decimals which was most satisfactory.

The influence line for the moment at junction 3 for instance is calculated as follows.

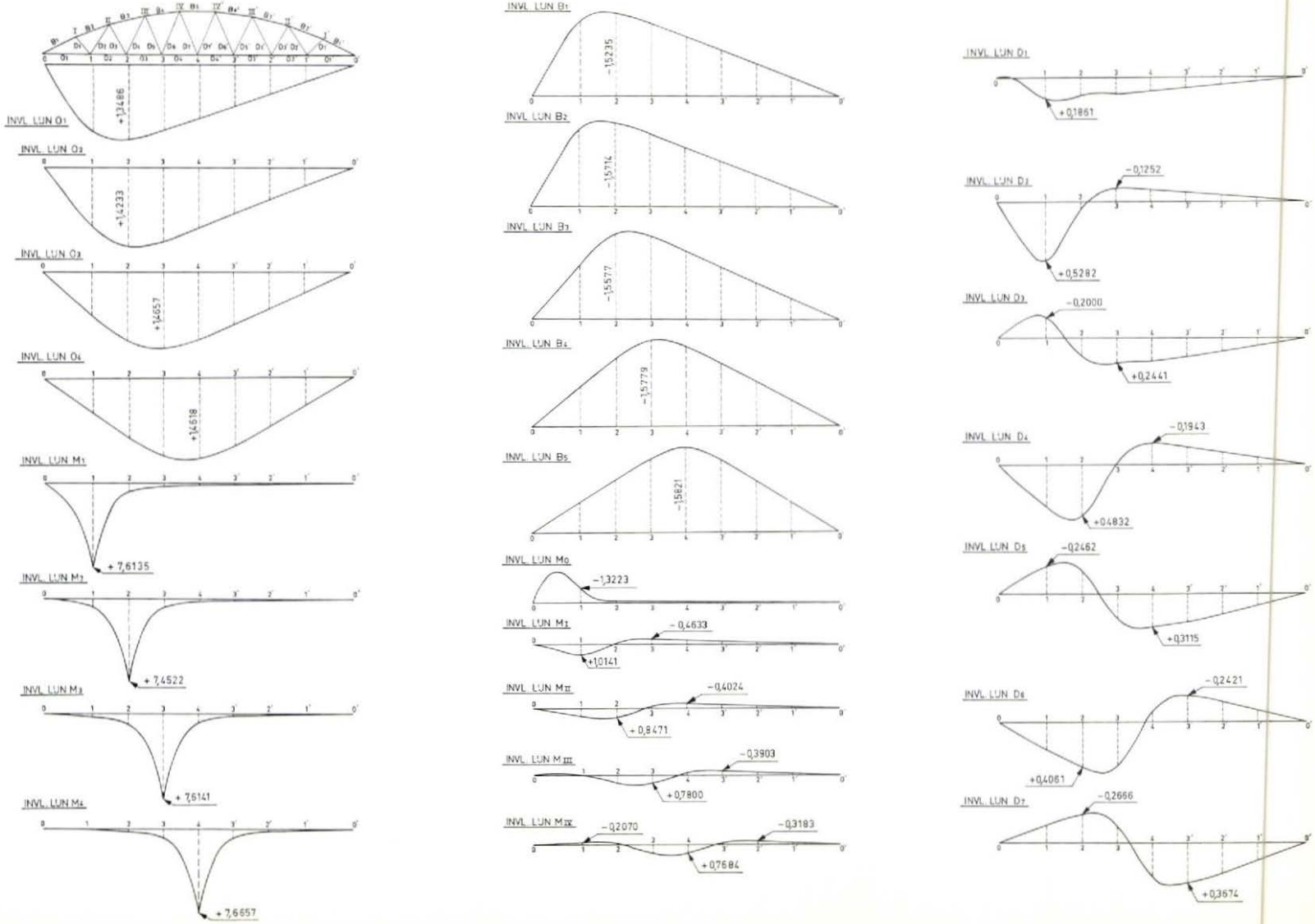

INVL. LUN O1
+13486
INVL. LUN O2
+14233
INVL. LUN O3
+14657
INVL. LUN O4
+14618
INVL. LUN M1
+ 7,6135
INVL. LUN M2
+ 7,4522
INVL. LUN M3
+ 7,5141
INVL. LUN M4
+ 7,6657
INVL. LUN B1
-15235
INVL. LUN B2
-15714
INVL. LUN B3
-15577
INVL. LUN B4
-15779
INVL. LUN B5
-15821
INVL. LUN M0
-1,3223
INVL. LUN M1
- 0,4633
+1,0141
INVL. LUN MII
-0,4024
+ 0,8471
INVL. LUN M III
-0,3903
+0,7800
INVL. LUN M IV
-0,2070
-0,3183
+0,7684
INVL. LUN D1
+0,1861
INVL. LUN D2
-0,1252
+0,5282
INVL. LUN D3
-0,2000
+0,2441
INVL. LUN D4
-0,1943
+04832
INVL. LUN D5
-0,2462
+0,3115
INVL. LUN D6
-0,2421
+0,4061
INVL. LUN D7
-0,2666
+0,3674

Figure V-3

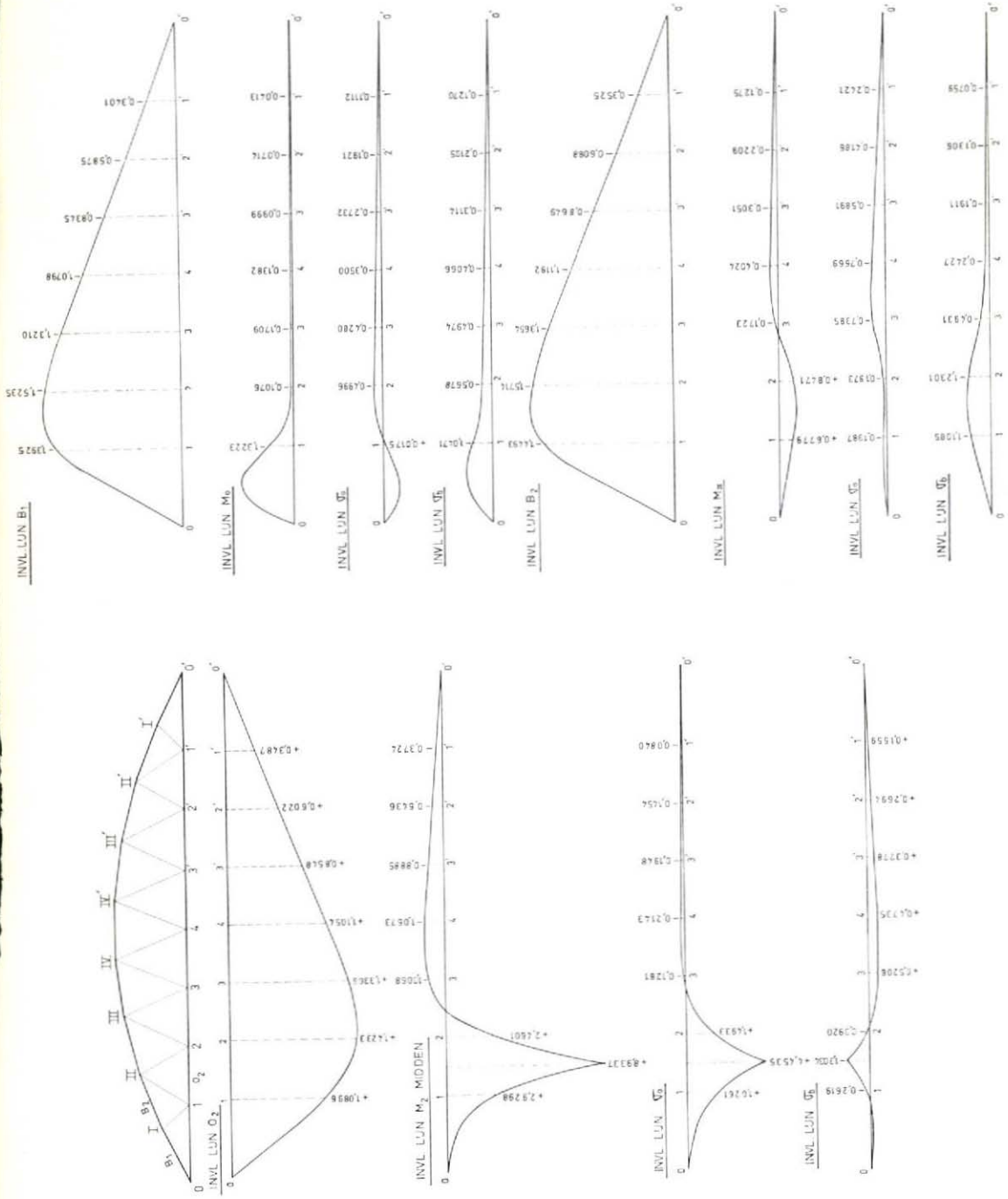

INVL LUN B1
INVL LUN Mo
INVL LUN
INVL LUN
INVL LUN B2
INVL LUN Mm
INVL LUN
INVL LUN
I
II
III
IV
V
VI
VII
INVL LUN O2
INVL LUN M2 MIDDEN
INVL LUN
INVL LUN

Figure V-4

The main girder consisting of arch and bottom chord, is assumed to have a hinge at junction 3 and the two equal but opposite moments of unity are applied at that point in the usual manner, one moment acting to the left and the other of opposite direction to the right. The other bending moments are then calculated with the aid of the matrix. The deflection curve of the bottom chord then represents the influence line while the diagram scale multiplication factor is the reciprocal of the angular deviation at 3 in radians.

To determine the normal force in a member, the influence line is computed by extending the member concerned by unity and calculating all the moments with the aid of the matrix, whereupon the deflection curve of the bottom chord can be computed, which gives the influence line direct to a scale of 1:1.

It should be mentioned here that the bottom chords are loaded eccentrically and that the effects of eccentricity have been taken into account from the outset, which complicates matters in no small measure and calls for a great deal more calculation.

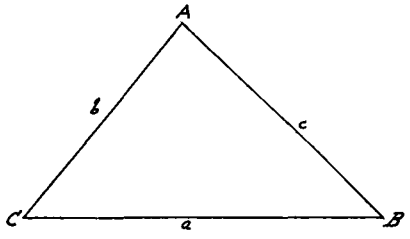
Figure V-3 shows the influence lines for the forces in the members and the moments at the junctions without the eccentricity effect of the forces in the truss.

The influence lines for the bending moments at the sections located in between two junctions of the girder can then be deduced from the influence lines for the bending moments at the junctions in the usual manner, in which also the effect of the eccentric forces must be incorporated (see Figure V-4).

Figure V-4 shows the influence lines for the stresses in the upper and lower fibres of the arch and bottom chord sections obtained by means of the influence lines for the direct forces and bending moments.

The influence lines for the forces including all the effects and approximations, computed in two different ways are seen to tally to four places of decimals, i.e. to 0.1 Kg, which is an encouraging result.

There are several methods by which the deformation of the truss may be calculated; the one found to be most effective is described below.



If ε_a, ε_b and ε_c are the specific elongations of the elements a, b and c of a triangular truss section, the angular deviations at A, B C are

$$\Delta_A = \varepsilon_a(\cot gB + \cot gC) - \varepsilon_b \cot gC - \varepsilon_c \cot gB$$
$$\Delta_B = \varepsilon_b(\cot gA + \cot gC) - \varepsilon_a \cot gC - \varepsilon_c \cot gA$$
$$\Delta_C = \varepsilon_c(\cot gA + \cot gB) - \varepsilon_a \cot gB - \varepsilon_b \cot gA$$

It is clear that the angular deviation for example at junction 3 (see Figure V-1) between members 3-2 and 3-4 equals

$$\Delta_{2\text{-}3\text{-}III} + \Delta_{III\text{-}3\text{-}IV} + \Delta_{IV\text{-}3\text{-}4}$$

i.e. the sum of the angular deviations in all three angles at point 3.

The deflection curve of the bottom chord for each degree of loading can be found by regarding the angular deviation between the members at the various junctions as forces and determining the bending moment diagram due to these forces. The latter then represents the deflection curve of the bottom chord.

If we look at Figure III-2 (Appendix III), we can easily see that the relationship between deflection and change in angle in a combination of hinged members is equal to

$$\Delta^2 y_n = -c\,\varphi_n$$

and it is also true that

$$\Delta^2 M_n = -c\,P_n \qquad \text{(see Appendix III)}$$

Of all the methods tried, the one described above is the most accurate, since it involves the smallest accumulation of any errors that may occur as a result of approximation.

With regards to the 2nd order theory, it can be said that the calculations have been made for maximum deformation of the truss, i.e. for maximum live loading.

Since the method of calculation is very insensitive to deformations due to live loading, there is no point in making three separate computations, one for the structure's dead load, one for its dead load + half of the live load and one for its dead load + the entire live load. That would mean three times the amount of work for practically identical results.

In the series of Rijkswaterstaat Communications the following numbers have been published before:

Nr 1 *). J. J. Dronkers and J. C. Schönfeld:
Tidal Computations in Shallow Water
A. Waalewijn:
Report on Hydrostatic Levelling across the Westerschelde

Nr 2 *). Ir. H. Ph. van der Schaaf and P. Vetterli, Ing. Dipl. E.T.H.:
Computation of the Decca Pattern for the Netherlands Delta Works

Nr 3. Ir. A. J. P. van der Burgh, J. P. Bouwman and G. M. A. Steffelaar:
The Aging of Asphaltic Bitumen

Nr 4. Dr. L. F. Kamps †:
Mud Distribution and Land Reclamation in the Eastern Wadden Shallows

Nr 5. Ir. J. C. le Nobel:
Modern Construction of Wing-Gates

Nr 6. Board of the Zuyder Zee Works:
A Structure Plan for the Southern IJsselmeerpolders

Nr. 7. Ir. J. van der Kley:
The Use of Explosives for Clearing Ice

*) out of print

